Journal of Applied Pharmaceutical Science 2025. Article in Press
Available online at http://www.japsonline.com
DOI: 10.7324/JAPS.2025.240961
ISSN 2231-3354

Network pharmacology and molecular dynamics studies unveil the therapeutic mechanisms of *Zingiber officinale* against dyspepsia

Stefeny Theresia Simatupang[1], Doni Dermawan[1], Nadia[1], Santi Tan[1], Raymond Rubianto Tjandrawinata[1,2*]

[1]Department of Dexa Omic Sciences (Dexomics), Dexa Medica, South Tangerang, Indonesia.
[2]Center for Pharmaceutical and Nutraceutical Research and Policy (CPNRP), Atma Jaya Catholic University of Indonesia, South Jakarta, Indonesia.

ARTICLE HISTORY

Received on: 04/02/2025
Accepted on: 03/08/2025
Available Online: XX

Key words:
AKT1, bioactive compounds, EGFR, gastrointestinal disorders, molecular dynamics simulation, phytotherapy.

ABSTRACT

Dyspepsia, or indigestion, is a condition marked by discomfort in the upper gastrointestinal tract, and existing treatments for functional dyspepsia often yield limited results. This study investigates the potential of *Zingiber officinale* (ginger) in treating dyspepsia using network pharmacology and molecular dynamics approaches. A total of 31 bioactive compounds were identified, targeting 29 proteins associated with dyspepsia. Kyoto Encyclopedia of Genes and Genomes pathway enrichment analysis revealed 160 related pathways (p-value ≤ 0.05), including the phosphatidylinositol-3-kinase/Akt signaling pathway, gastric cancer, and nuclear factor kappa-light-chain-enhancer of activated B cells signaling pathway. A compounds–targets–pathways (C-T-P) network highlighted the central roles of epidermal growth factor receptor (EGFR) and Ras-related C3 botulinum toxin substrate–alpha serine/threonine-protein kinase (AKT1) in modulating inflammatory responses and proliferation of gastrointestinal epithelial cells, with significant implications in the pathogenesis of gastrointestinal disorders, validated via molecular docking. Compounds such as 3,5-diacetoxy-1-(4-hydroxy-3,5-dimethoxyphenyl)-7-(4-hydroxy-3-methoxyphenyl)heptane (DDMHMH), alpha-tocopherol, gingerol, and shogaol showed good binding ($\Delta G_{binding} < -5.00$ kcal/mol). Molecular dynamics simulations for 50 ns confirmed the stability of DDMHMH–AKT1 and DDMHMH–EGFR complexes. Binding free energy (Molecular mechanics/Poisson–Boltzmann surface area) calculations supported strong interactions, with $\Delta G_{binding}$ values of −8.71 kcal/mol (AKT1–DDMHMH) and −11.44 kcal/mol (EGFR–DDMHMH). These findings support *Z. officinale's* potential for dyspepsia therapy.

INTRODUCTION

Dyspepsia, often described as indigestion, is a medical condition encompassing a spectrum of discomfort or pain in the upper gastrointestinal tract [1,2]. This prevalent gastrointestinal disorder in medical practice exerts a significant global impact, affecting millions and resulting in substantial healthcare costs, work absenteeism, and decreased quality of life for patients [3]. Dyspepsia is classified into two main categories: organic and functional dyspepsia (FD). Organic dyspepsia arises from identifiable pathological causes such as peptic ulcers, gastroesophageal reflux disease, gastrointestinal malignancies, pancreatic or biliary disorders, and drug or food intolerance [2]. In contrast, FD is diagnosed when no observable organic cause is found despite persistent symptoms such as postprandial fullness, early satiety, and epigastric pain [4]. The development of FD involves various factors, including dietary factors, psychological stress, disruptions in gastric physiology, duodenal inflammation, and infections like *Helicobacter pylori* [5].

The standard treatment for FD includes *H. pylori* eradication drugs, improving gastrointestinal motility, alleviating visceral hypersensitivity, and addressing anxiety and depression. However, their limited efficacy, risk of adverse effects, and high recurrence rates highlight a therapeutic gap [4,6]. Consequently,

*Corresponding Author
Raymond Rubianto Tjandrawinata, Department of Dexa Omic Sciences (Dexomics), Dexa Medica, South Tangerang, Indonesia. E-mail: raymond @ dexa-medica.com

there is an increasing interest in complementary and alternative approaches, particularly herbal medicines, which are deeply rooted in traditional medical systems, especially in Asia. *Liu Jun Zi Tang*, also known as Rikkunshito, has been recognized since the 16th century for treating dyspepsia [6]. Accordingly, experts anticipate that herbal medicines will emerge as safe therapeutic options for FD [7]. Herbal medicines such as ginger, licorice, papaya, peppermint oil, caraway oil, and activated charcoal have been widely studied for managing FD [8]. Additionally, related studies on gastrointestinal disorders have shown promise in demonstrating the therapeutic potential of herbal medicines. For example, the bioactive fraction DLBS2411 from *Cinnamomum burmanni* (cinnamon) effectively reduced ulcer size and severity in a rat model of peptic ulcers, with efficacy comparable to omeprazole or sucralfate, and a good safety profile [9,10].

Ginger (*Zingiber officinale*) is a perennial rhizomatous plant of the Zingiberaceae family, recognized for its widespread application as a culinary spice, seasoning, and herbal remedy [11]. Ginger has been widely recognized as a traditional dietary remedy for alleviating gastrointestinal symptoms such as nausea, bloating, and indigestion, making it a beneficial option for managing FD. In addition to these effects, ginger's potential to stimulate appetite, enhance metabolic activity, and modulate gut microbiota further underscores its multifaceted role within contemporary nutritional and gastrointestinal research [12]. Gastric ulcers can be caused by various factors, including *H. pylori* infection, hydrochloric acid, pepsin, alcohol, and the use of nonsteroidal anti-inflammatory drugs [13]. Ginger has shown effectiveness in preventing gastric ulcers induced by these factors [14]. Several studies have demonstrated ginger's anti-inflammatory, antioxidant, antitumor, and anti-ulcer effects. Its biological effects include the presence of phenolics, such as gingerols, shogaol, paradol, and zingerone, as well as monoterpenes like limonene and citral. Among these components, gingerols and shogaols are identified as the most active ingredients [15,16]

The traditional 'one drug-one target-one disease' paradigm is challenged by complex conditions like dyspepsia, which are driven by a wide range of biological processes (BPs) and molecular functions (MFs). To address this, network pharmacology can be employed to elucidate the therapeutic mechanisms of drugs at the biological targets and pathways levels, aligning seamlessly with the complexity of traditional Chinese medicine (TCM), characterized by multi-component, multi-targeted, and integrative efficacy [17]. For instance, network pharmacology has been conducted to investigate the therapeutic effects of various herbal plants, including the immunomodulatory properties of *Astragali radix* (Huangqi) [18], the antidiabetic potential of *Lagerstroemia speciosa* and *C. burmanni* in type 2 diabetes [19], and the hepatoprotective activity of *Phyllanthus niruri* [20]. The present study aims to investigate the therapeutic mechanisms of *Z. officinale* against dyspepsia using an integrative approach that combines network pharmacology, molecular docking, and molecular dynamics simulation (MDS). The results of this study may contribute to the development of ginger-based therapeutic agents for

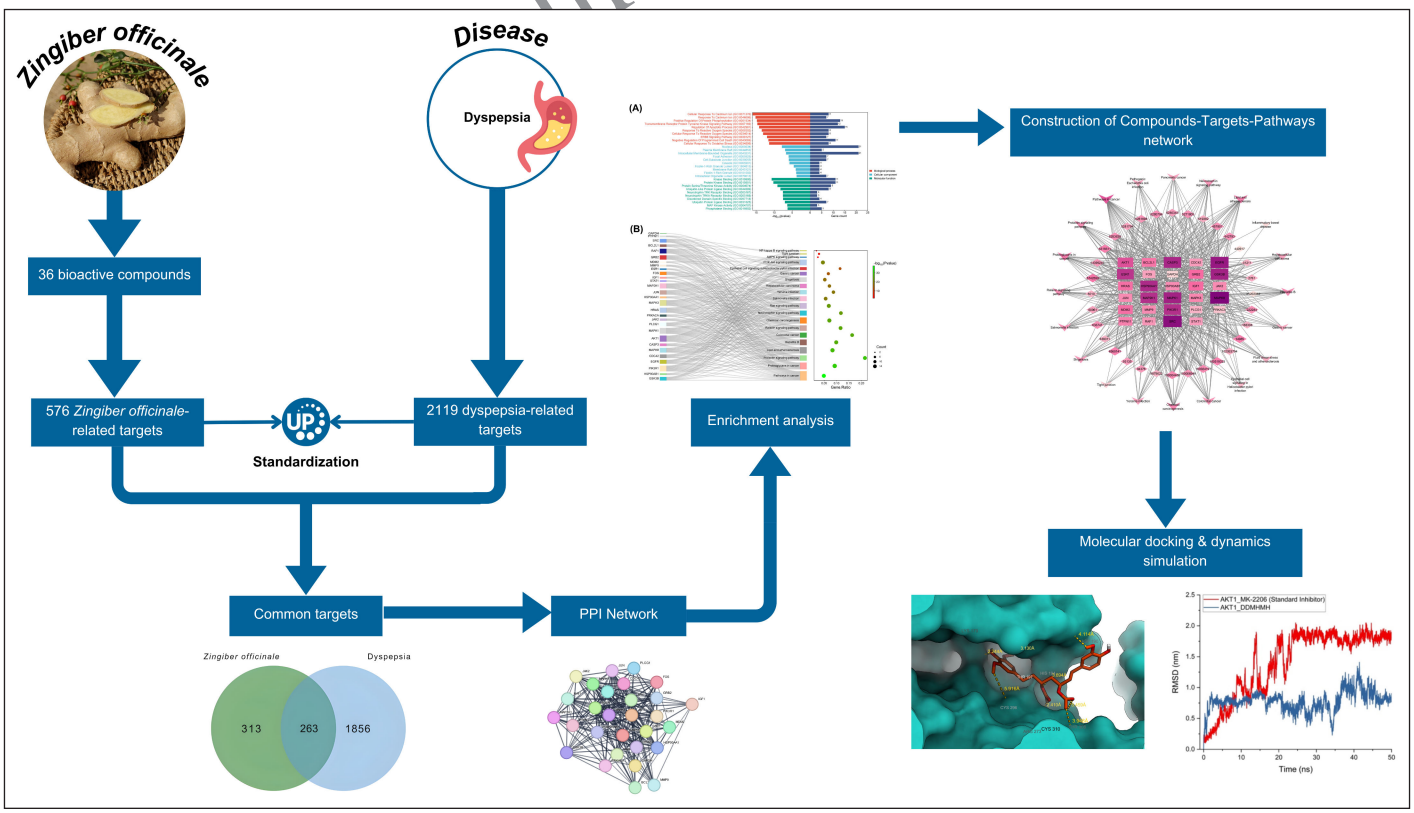

Figure 1. The workflow diagram of network pharmacology, molecular docking, and MDS of *Z. officinale* concerning dyspepsia.

functional gastrointestinal disorders. Figure 1 illustrates the study's workflow graphically.

MATERIALS AND METHODS

Data collection and screening of bioactive compounds

We collected compounds of *Z. officinale* from literature sources [16,21,22] and databases, including Bioinformatic Analysis Tool for Molecular Mechanism of Traditional Chinese Medicine (BATMAN-TCM, http://bionet.ncpsb.org.cn/batman-tcm/) [23] and Traditional Chinese Medicine Systems Pharmacology Database and Analysis Platform (TCMSP, https://old.tcmsp-e.com/tcmsp.php) [24]. These compounds underwent screening using a threshold of ≥30% for oral bioavailability (OB) and ≥0.18 for drug-likeness (DL) values, resulting in bioactive compounds fit for further analysis [25]. We used SwissADME (http://www.swissadme.ch/index.php) to predict the OB properties of the compounds and the MolSoft database (https://www.molsoft.com/) to predict the DL properties of the compounds, with these steps involving the insertion of the compounds' canonical simplified molecular input line entry system (SMILES) [26,27]. We retrieved information, such as the compound's molecule name, PubChem CID, and canonical SMILES, from the PubChem database (https://pubchem.ncbi.nlm.nih.gov/) [28].

Data collection and screening of target proteins

Target proteins linked to *Z. officinale* were collected and limited to *Homo sapiens* (human) only, using the PharmMapper server (https://www.lilab-ecust.cn/pharmmapper/) and Similarity ensemble approach database (SEA, https://sea16.docking.org/) [29,30]. Targets from the PharmMapper server were collected by inputting the compounds' 2D structure data file format from the PubChem database. We only chose targets with a *z*' score with a positive value. Meanwhile, targets from the SEA database were collected by inputting the canonical SMILES of the bioactive compounds and choosing targets with a Tanimoto coefficient of ≥0.5. We also used the Research Collaboratory for Structural Bioinformatics (RCSB) Protein Data Bank (RCSB PDB, https://www.rcsb.org/) to complement the ligand mapping provided by PharmMapper. Furthermore, we excluded the duplicate targets and used the UniProt database (https://www.uniprot.org/) to standardize the identified target proteins [31–33].

Targets linked to dyspepsia were collected using the search keyword "dyspepsia" from the GeneCards database (https://www.genecards.org), the National Center for Biotechnology Information Gene (NCBI Gene, https://www.ncbi.nlm.nih.gov/gene/), and Disease Gene Network version 7.0 (DisGeNET, https://www.disgenet.org/). We excluded duplicate identified targets, standardized the targets using UniProt, and employed the JVenn program (https://jvenn.toulouse.inra.fr/app/example.html) to illustrate the intersection of targets between *Z. officinale* and dyspepsia [34–37].

Construction of protein-protein interaction (PPI) network

We constructed PPI networks for targets linked to *Z. officinale*, dyspepsia, and their common targets using the stringApp within the Cytoscape software version 3.10.2 (https://cytoscape.org/) for visualization [38,39]. The species type selected was *H. sapiens*, with a confidence level set at 0.700 for reliability values, while the rest remained at default settings. Common targets were identified by intersecting PPI networks associated with *Z. officinale* and dyspepsia. Additionally, we employed CytoNCA tools within Cytoscape software to analyze the PPI network results and assess network topology parameters, including degree centrality (DC), eigenvector centrality, betweenness centrality (BC), and closeness centrality (CC) of targets [40]. We used these findings to identify essential nodes in the network by selecting target nodes with values surpassing the respective median values in the PPI network. Subsequently, we utilized the selected target nodes to form a new network comprising crucial targets linked to *Z. officinale* and dyspepsia [41].

Enrichment analysis

We employed Gene Ontology functional annotations (GO, https://www.geneontology.org/) and the Kyoto Encyclopedia of Genes and Genomes database (KEGG, https://www.genome.jp/kegg/pathway.html) for the crucial targets linked to *Z. officinale* and dyspepsia using Enrichr (https://maayanlab.cloud/Enrichr/) as the enrichment analysis tool [42]. The GO database can examine BPs, MFs, and cellular components (CCs) [43]. Meanwhile, KEGG was employed to acquire the signaling pathways associated with *Z. officinale* and dyspepsia [44]. We also visualized the top 10 GO terms and KEGG pathways using SRplot (https://bioinformatics.com.cn/) according to the smallest *p*-value to draw bar graphs and Sankey diagrams [45,46].

Construction of the C-T-P network

The C-T-P network, which illustrates the interaction between bioactive compounds, crucial targets, and signaling pathways involved in *Z. officinale* for dyspepsia, was constructed using Cytoscape version 3.10.2 [39]. Within this network, biological nodes represent potential bioactive compounds, crucial targets, and signaling pathways, while edges illustrate their interactions. The significance of a target in this network is assessed by its DC, indicating the number of connections it has with other targets. Targets with higher DC exhibit more robust connectivity and influence the overall network of bioactive compounds and pathways [47].

Molecular docking

Potential bioactive compounds identified from the C-T-P network with high DC were selected as the ligands for molecular docking against crucial targets using the High Ambiguity Driven Protein-Protein Docking (HADDOCK, https://rascar.science.uu.nl/haddock2.4/) web server version 2.4 [48]. The three-dimensional structures of epidermal growth factor receptor (EGFR) (PDB ID: 1M17) at a resolution of 2.60 Å (chain A) [49] and RAC-alpha serine/threonine-protein kinase (AKT1) (PDB ID: 3O96) at a resolution of 2.70 Å (chain A) were retrieved from RCSB PDB [32]. In contrast, the two-dimensional structures of ligands were obtained from PubChem [28]. Heteroatoms were removed from protein structures using

BIOVIA Discovery Studio (https://discover.3ds.com/discovery-studio-visualizer-download) [50]. In cases where the structure exhibited disruptions due to missing amino acid residues, the corresponding corrected models were sourced from the AlphaFold Protein Structure Database (https://alphafold.ebi.ac.uk/) [51]. Furthermore, the Computed Atlas of Surface Topography of the universe of protein Folds (CASTpFold, https://cfold.bme.uic.edu/castpfold/) [52] was employed to predict the ligand-binding domains based on these structures.

Ligand structures were prepared and geometrically optimized using Chem3D with MM2-based energy minimization to reduce steric strain and refine bond angles and lengths [53]. To serve as reference compounds, two standard ligands were incorporated: Erlotinib, a recognized EGFR inhibitor [54], and MK-2206, an AKT1 inhibitor [55]. Both ligands were also subjected to MM2 energy minimization to ensure uniform preparation across all docking analyses. Protein Data Bank summary (https://www.ebi.ac.uk/thornton-srv/databases/pdbsum/) was used to determine the ligand-binding domains by entering the relevant PDB ID [56]. Furthermore, binding affinities (ΔG) in kcal/mol of the docked complexes were predicted using PRODIGY-LIGAND (PROtein binDIng enerGY prediction, https://rascar.science.uu.nl/prodigy/) [57], with more negative values indicating stronger protein-ligand interactions [58]. The 2D structures of the complexes were visualized using BIOVIA Discovery Studio, while the 3D structures were visualized using UCSF ChimeraX (https://www.rbvi.ucsf.edu/chimerax/) [59].

Molecular dynamics simulation

To investigate the dynamic behavior, conformational stability, and binding interactions of the top-performing ligand with target receptors AKT1 and EGFR, MDS were conducted using GROMACS 2024.3 [60]. Ligand topologies were generated with GAFF2 parameters, and atomic partial charges were assigned using the AM1-BCC method via ACPYPE integrated with AmberTools21. The CHARMM27 force field was applied to the protein receptors, while the TIP3P water model was used for solvation within a triclinic simulation box, maintaining a 1.0 nm buffer distance. The ligand and receptor coordinates were merged and verified using UCSF Chimera, with subsequent topology file modifications to ensure correct inclusion of ligand parameters. The system was solvated using the SPC216 water model, neutralized with counterions, and adjusted to 0.1 M NaCl concentration to mimic physiological ionic strength.

Energy minimization was performed using the steepest descent algorithm to remove steric clashes. Equilibration was carried out in two phases: an number of particles (N), system volume (V) and temperature (T) are constant / conserved) ensemble phase using a Berendsen thermostat at 310 K, followed by an number of particles (N), system pressure (P) and temperature (T) are constant / conserved) phase using the Berendsen barostat at 1 bar. Position restraints were applied to both protein and ligand during equilibration to maintain initial conformations. Index files were generated to define restraint groups accurately. Finally, a 50 ns production run was performed under unrestrained conditions using the V-rescale thermostat and Parrinello–Rahman barostat for temperature and pressure control, respectively. Long-range electrostatics were handled using the Particle Mesh Ewald method, and a 1.2 nm cutoff was used for van der Waals interactions, enabling a detailed analysis of the ligand–receptor complex dynamics.

Molecular mechanics/Poisson–Boltzmann surface area (MM/PBSA) calculations

To estimate the binding free energy of the top-performing ligand with the AKT1 and EGFR receptors, MM/PBSA calculations were performed using the gmx_MMPBSA module [61]. This approach provided a quantitative evaluation of the binding affinity by combining molecular mechanics energies with solvation energies obtained from continuum electrostatics. Trajectory files from the 50-ns molecular dynamics (MD) production run were utilized, and representative snapshots were extracted at regular intervals for post-processing. The MM/PBSA calculations included van der Waals, electrostatic, polar solvation, and non-polar solvation energy components, with solvent-accessible surface area used to approximate non-polar contributions. The analysis was executed with default dielectric constants and grid spacing parameters optimized for protein–ligand complexes, enabling robust and accurate estimation of binding energetics critical for validating ligand–receptor interactions observed during MDS.

RESULTS AND DISCUSSION

Data collection and screening of bioactive compounds

Based on previous phytochemical studies and databases, such as BATMAN-TCM and TCMSP, 477 compounds were retrieved (Supplementary Table S1 for detailed information). In TCM, compounds must possess appropriate pharmacokinetic characteristics to effectively reach target organs and exert their biological effects [62]. OB is a component of the absorption, distribution, metabolism, and excretion parameters, which serves as an indicator of a compound's potential efficacy. Compounds with an OB value of ≥30% are generally considered to exhibit favorable DL [63]. Furthermore, DrugBank reports an average DL index of 0.18, and compounds with a DL value of 0.18 or higher are therefore considered to exhibit high druggability [62]. Upon screening using a threshold of ≥30% for OB and ≥0.18 for DL values, 36 bioactive compounds were selected as potential bioactive compounds for further analysis (as detailed in Supplementary Table S2). Retained for consideration among potential bioactive compounds were shogaol, paradol, zingerone, gingerol, citral, and limonene, all known for their therapeutic potential in gastrointestinal diseases, supported by previous studies.

Data collection and screening of target proteins

Targets corresponding to the 36 bioactive compounds of *Z. officinale* were retrieved from the SEA and PharmMapper databases, yielding 576 targets following the removal of duplicates (Supplementary Tables S3 and S4 for comprehensive data). Concurrently, targets linked to dyspepsia were retrieved from the GeneCards, NCBI Gene, and DisGeNET

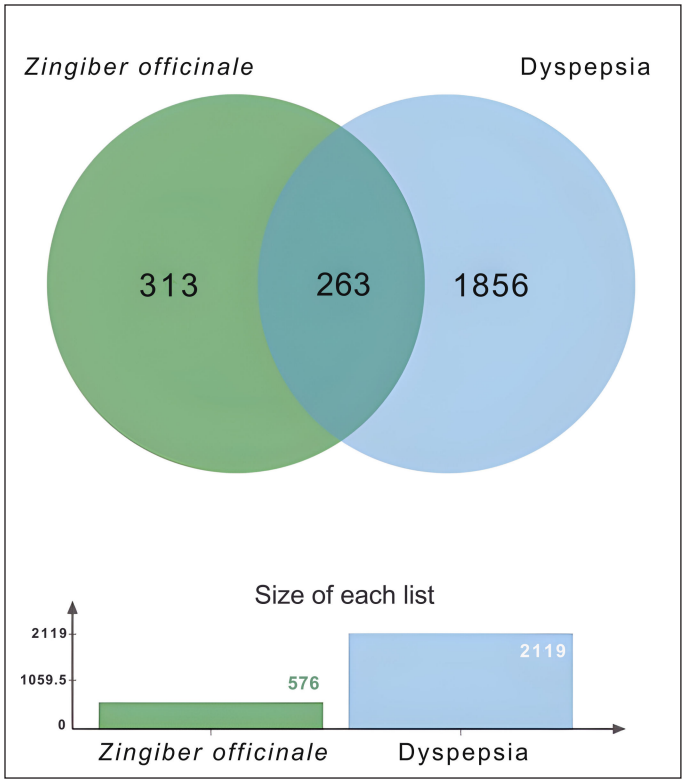

Figure 2. Venn diagram illustrating common targets between *Z. officinale* and dyspepsia. The green circle denotes *Z. officinale* targets, while the blue circle signifies dyspepsia targets.

databases, resulting in 2,119 targets after removing duplicates (Supplementary Table S5). The intersection of unique *Z. officinale* and dyspepsia targets led to the identification of 263 common targets, as delineated in Supplementary Table S6. Figure 2 represents these shared targets as a Venn diagram generated using the JVenn program.

PPI network

We constructed the PPI network using stringApp within Cytoscape software version 3.10.2. The PPI network of *Z. officinale* targets contained 571 nodes and 2,423 edges, representing 576 listed genes. Concurrently, the PPI network of dyspepsia targets contained 2,108 nodes and 26,939 edges, representing 2,119 listed genes. The merging intersection of both PPI networks resulted in a common target PPI network, comprising 262 nodes and 1,290 edges, representing 263 listed genes. Figure 3 shows these PPI networks. Additionally, the common targets network underwent analysis using CytoNCA within Cytoscape software version 3.10.2, resulting in 74 potential and 29 crucial targets identified through tiered screening based on topological parameters such as DC, EC, BC, and CC ≥ their median. We selected the identified 74 potential targets from the common targets to gather the crucial compounds from the study. Supplementary Tables S7–S10 provide detailed information. Among 36 bioactive compounds, 3,5-diacetoxy-1-(4-hydroxy-3,5-dimethoxyphenyl)-7-(4-hydroxy-3-methoxyphenyl)heptane (DDMHMH) (PubChem CID: 5316611) was the most potent compound with the

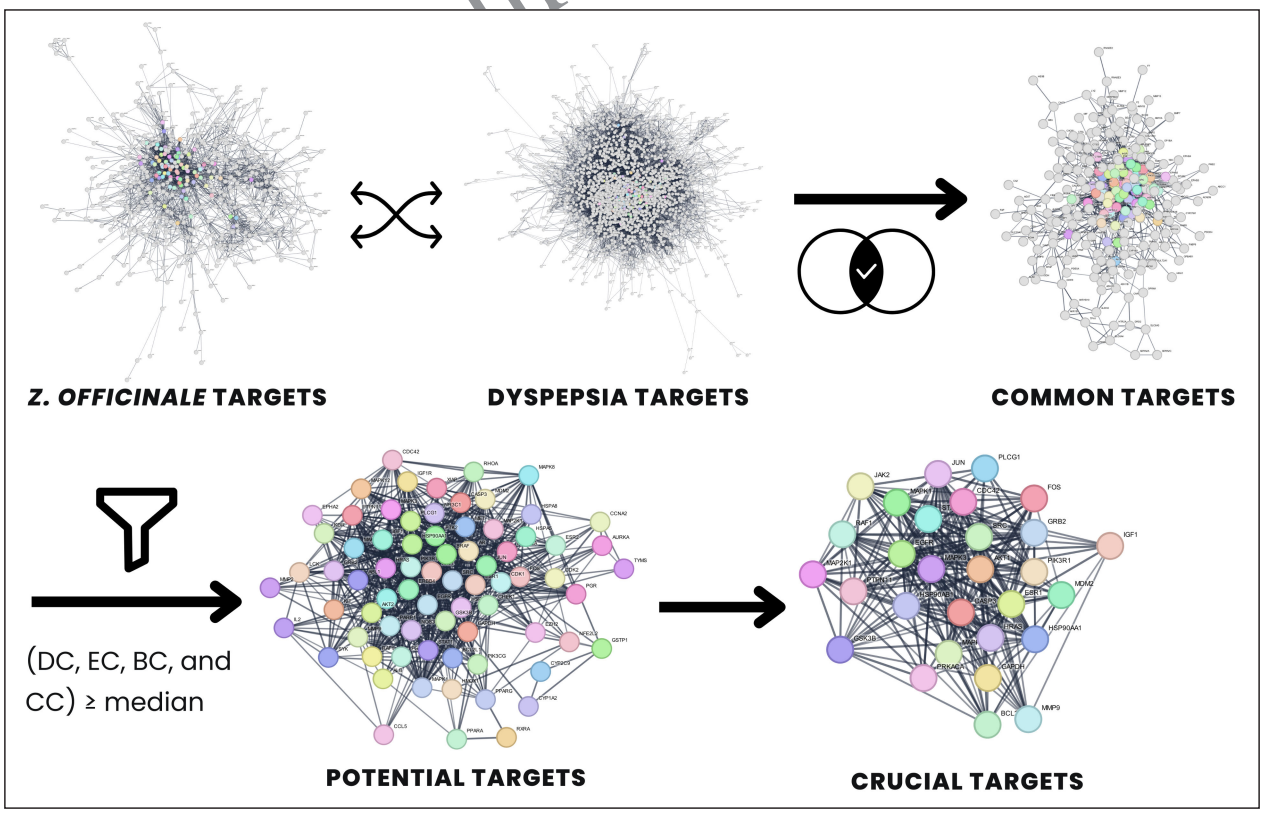

Figure 3. Construction of PPI networks.

highest DC of 50.00, followed by (2R)-2-[[2-[2-chloro-N-methylsulfonyl-5-(trifluoromethyl)anilino]acetyl]-[(3-methoxyphenyl)methyl]amino]-N-propylpropanamide with DC of 49.00 and alpha-tocopherol (PubChem CID: 14985) with DC of 48.00. However, (2R)-2-[[2-[2-chloro-N-methylsulfonyl-5-(trifluoromethyl)anilino]acetyl]-[(3-methoxyphenyl)methyl] amino]-N-propylpropanamide has not been previously reported or studied in the context of dyspepsia or any gastrointestinal disease. Additionally, aromatic compounds like gingerols (PubCHem CID: 442793) and shogaols (PubChem CID: 5281794) are the most active in *Z. officinale* [64], exhibiting a high DC of 44.00. Therefore, we selected these compounds for molecular docking.

DDMHMH, the most potent bioactive compound found in ginger, belongs to the class of diarylheptanoids, is one of the more significant phenolic compounds commonly present in ginger [65]. Diarylheptanoids exhibit a complex phenolic structure, comprising two aromatic rings linked by a seven-carbon chain. These compounds contribute to the organoleptic characteristics of ginger. Renowned for their diverse pharmacological activities, diarylheptanoids possess anti-inflammatory, anti-ulcer, anti-cathartic, antiemetic, diuretic, choleretic, hepatoprotective, cholesterol-lowering, antibacterial, antifungal, analeptic, and antidiabetic properties [66]. The potent anti-ulcer properties of diarylheptanoids might be attributed to their notable anti-inflammatory and antioxidant effects [66,67]. Research by Tao *et al.* [68] revealed that diarylheptanoids isolated from *Z. officinale* can inhibit the formation of lipid peroxides in liver microsomes and effectively scavenge superoxide anion radicals. Through their antioxidant

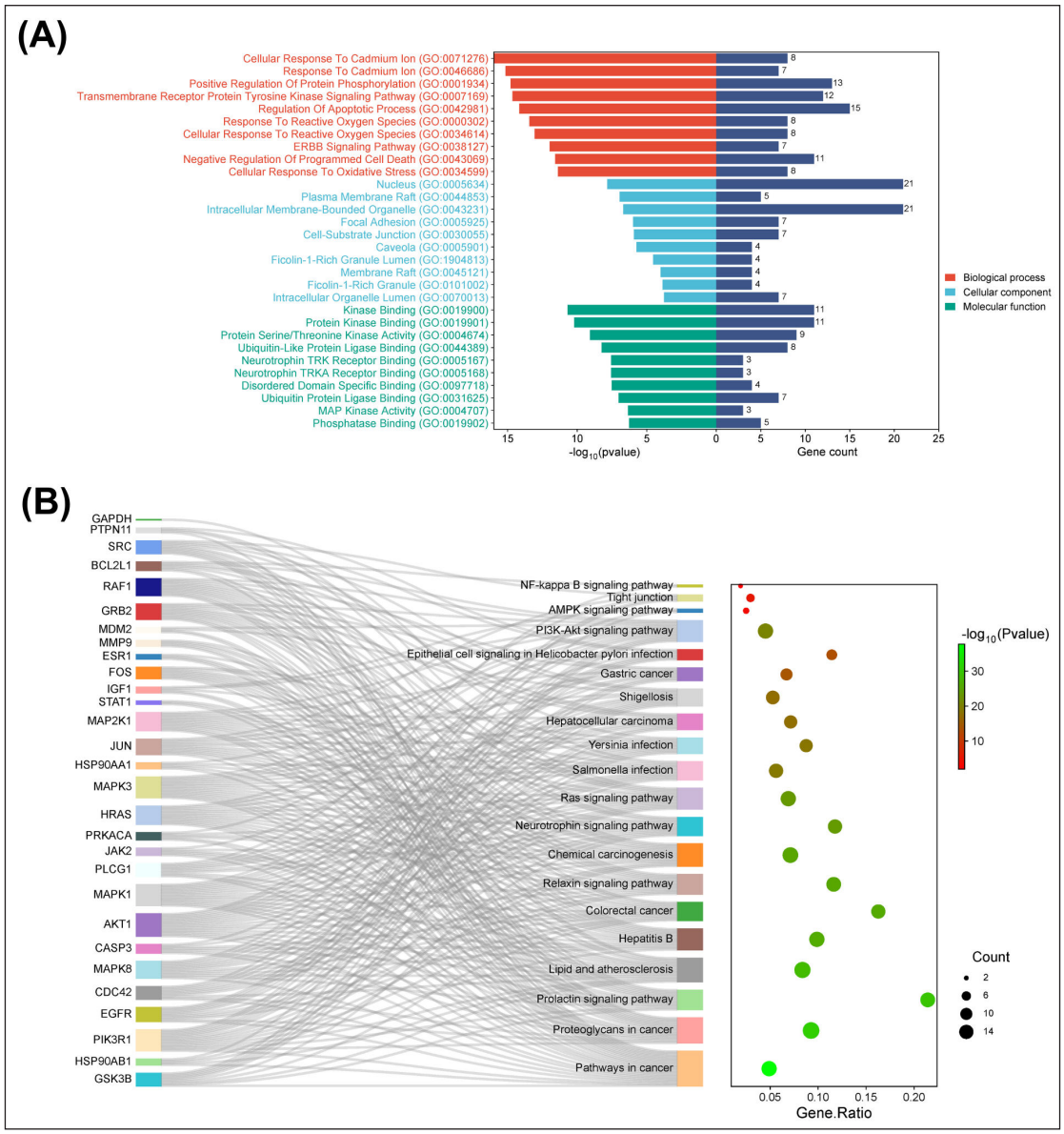

Figure 4. Enrichment analysis of the crucial targets. (A) Bar graph of top 10 enriched BPs, MFs, and CCs. (B) Sankey diagram with a bubble plot illustrating 20 KEGG pathways. *BPs = biological processes, MFs = molecular functions, CCs = cellular components.

actions, diarylheptanoids may offer protection against gastric ulceration by counteracting reactive free radicals implicated in gastric mucosal damage, thereby mitigating the risk of ulcer development [67].

Alpha-tocopherol, a form of vitamin E, has demonstrated gastroprotective properties against the development of gastric lesions. Observations show that alpha-tocopherol can mitigate the harmful effects of ulcerogenic agents by preserving the function of antioxidant enzymes within the stomach. This action shields the gastric tissue from oxidative stress, consequently reducing its susceptibility to ulcer formation. Furthermore, Huang *et al.* [69] research revealed that alpha-tocopherol also influences intestinal tight junctions, both *in vitro* and *in vivo*. Although alpha-tocopherol is not a primary constituent of ginger, it appeared as a high-DC node in our network because of its broad antioxidant role. A study by Ajith *et al.* [70]found that ginger extract (250–500 mg/kg) in combination with alpha-tocopherol provided better protection against cisplatin-induced kidney damage than either one alone. This suggests a synergistic effect between ginger and alpha-tocopherol [70].

Gingerol, recognized as the principal pungent constituent of ginger, exhibits a wide range of pharmacological properties. Belonging to a group of compounds that share a 3-methoxy-4-hydroxyphenyl core, gingerols are categorized into several forms, including shogaols, paradols, zingerone, gingerdiones, and gingerdiols. These bioactive molecules have been associated with multiple therapeutic effects, such as anticancer, antibacterial, blood glucose-regulating, liver and kidney-protective, gastrointestinal, neurological, and cardiovascular protective effects [71]. Gingerols are sensitive to heat and quickly dehydrate to form shogaols [14], providing gastroprotective benefits by maintaining the gut barrier. In animal models, an experimental study showed that shogaol preserves intestinal tight junctions and shields enteric dopaminergic neurons from 1-methyl-4-phenyl-1,2,3,6-tetrahydropyridine-induced damage [72]. A study also discovered that shogaol helps protect the gut barrier in Caco-2 and HT-29/B6 cells inflamed by tumor necrosis factor α (TNF-α). It does this by regulating tight junction-related proteins like claudin-2 and claudin-1 through the inhibition of NF-κB signaling [73].

Enrichment analysis

We conducted the enrichment analysis on the list of 29 crucial targets. The GO function enrichment analysis yielded 1,064 BPs, 152 MFs, and 76 CCs, as detailed in Supplementary Table S11. The top 10 entries of the GO function (with $p \leq 0.05$) for each annotation were visualized in a bar graph, as depicted in Figure 4A. Additionally, the KEGG pathway analysis identified 183 pathways, with the 20 selected pathways (with $p \leq 0.05$) illustrated in a Sankey diagram, presented in Figure 4B, and listed in Supplementary Table S12 for comprehensive details. This study identified 29 key targets, with AKT1 and EGFR showing the highest DC values of 52.00 and 48.00, respectively. 183 KEGG pathways were enriched, of which 160 exhibited a p-value ≤ 0.05. Notably, pathways such as the phosphatidylinositol-3-kinase/Akt (PI3K–Akt) signaling pathway (KEGG: 04151; p-value = 3.64×10^{-21}; FDR = 2.67×10^{-20}), gastric cancer (KEGG: 05226; p-value = 6.88×10^{-15}; FDR = 1.97×10^{-14}), epithelial cell signaling in *H. pylori* infection (KEGG: 05120; p-value = 6.03×10^{-14}; FDR = 1.49×10^{-13}), tight junction (KEGG: 04530; p-value = 4.09×10^{-6}; FDR = 5.94×10^{-6}), adenosine monophosphate-activated protein kinase (AMPK) signaling pathway (KEGG: 04152; p-value = 6.87×10^{-4}; FDR = 8.98×10^{-4}), and nuclear factor kappa-light-chain-enhancer of activated B cells (NF-κB) NF-κB signaling pathway (KEGG: 04064; p-value = 9.92×10^{-3}; FDR = 1.15×10^{-2}), were identified as potentially associated with dyspepsia in this study.

The PI3K–Akt pathway (refer to Fig. 5 for further details on the targets studied in this pathway) mainly involves AKT1 and EGFR. It is a well-conserved signaling network in eukaryotic cells that supports cell survival, growth, and progression through the cell cycle [74]. Akt1 is a serine/threonine kinase involved in the regulation of cell growth, survival, and proliferation [75]. EGFR is a transmembrane glycoprotein classified as a member of the receptor tyrosine kinase family. Although EGFR activation promotes wound healing, cell growth, proliferation, and differentiation, it has also been linked to the emergence of cancers, including gastric cancer [76]. EGFR is a crucial assessment marker for the efficacy of ulcer healing in gastrointestinal damage due to its protective function for the digestive tract mucosa. EGF specifically targets gastric mucosa cells, and binding to EGFR enhances the quality of ulcer healing and tissue repair [77].

Moreover, 6-shogaol (commonly referred to as shogaol in PubChem, CID: 5281794), a bioactive compound found in ginger, exhibits barrier-protective effects during intestinal inflammation by inhibiting the PI3K/Akt and NF-κB signaling pathways. It is known that the pro-inflammatory cytokine TNF-α can induce barrier loss by upregulating claudin-2, a channel-forming tight junction protein, and attenuating claudin-1, a sealing tight junction protein. The analysis of PI3K/Akt signaling showed that 6-shogaol inhibited the TNF-α-induced phosphorylation of Akt Thr308 [78]. Shogaol inhibits the PI3K/AKT/mTOR pathway by directly inhibiting AKT1 and AKT2 by binding to an allosteric location at a lower interface amid the N- and C-lobes of the kinase domain [79].

Through network pharmacology analysis, we identified several pathways, which are classified under "pathways in cancer" that are influenced by active compounds in *Z. officinale* [80]. Although FD is non-malignant, the molecular mechanisms inferred from these cancer-related pathways are relevant. Such pathways control cell adhesion, migration, and barrier integrity, features critical for gastric mucosal homeostasis and integrity. The development of gastric cancer (Fig. 6 for further details on the targets studied in this pathway) is intricately linked to AKT1, an isomer of protein kinase B (AKT) [81]. Researchers have found that the upstream molecules of the PH domain leucine-rich repeat protein phosphatase 2 and the phosphatase and tensin homolog of Akt1 protein control its phosphorylation. Dysregulation of the PI3K/Akt/mTOR pathway is extensively observed in human cancer [82], including gastric cancer, which arises from numerous genetic and epigenetic alterations [83]. Exposure of cancer cells to harmful substances like cadmium

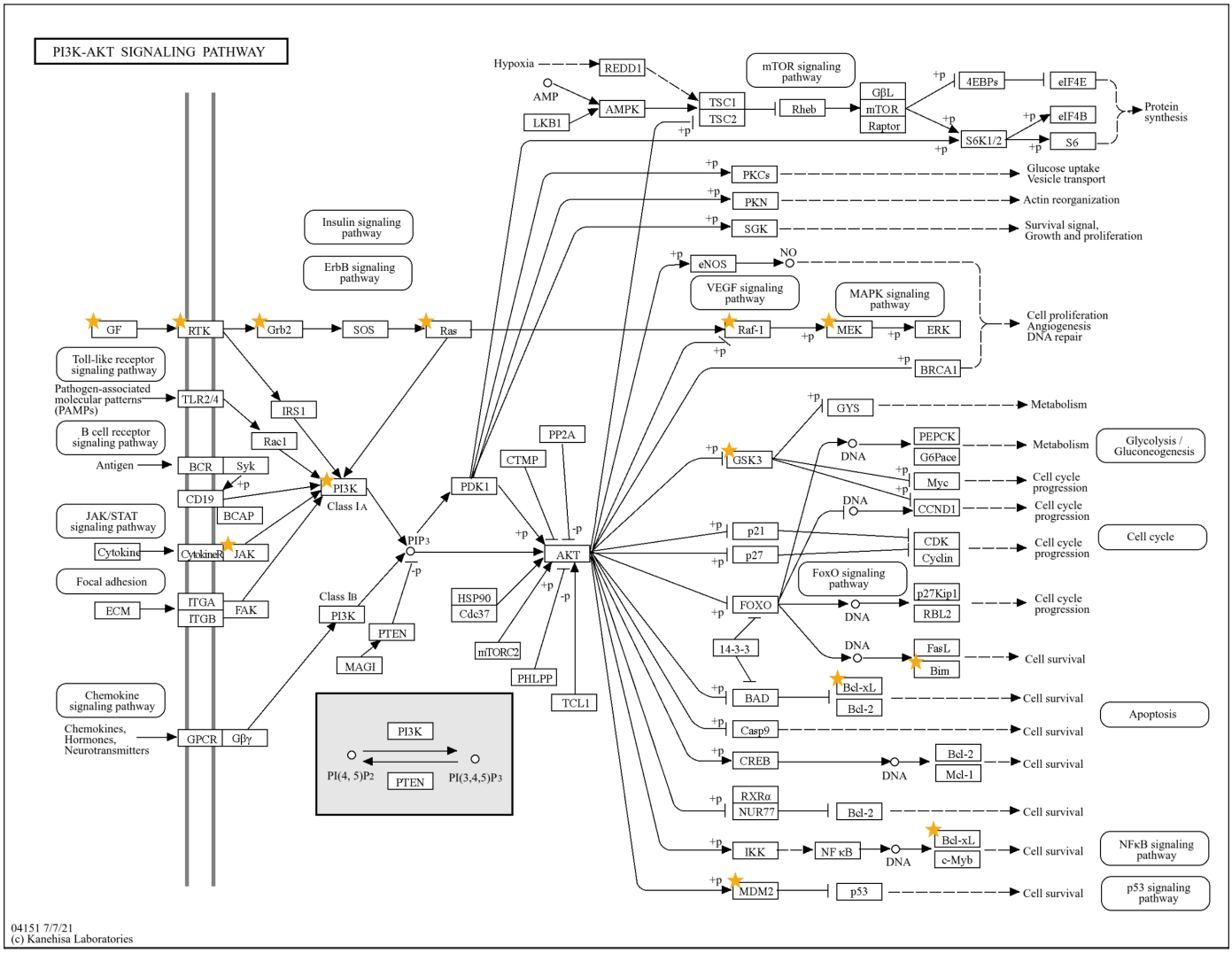

Figure 5. KEGG pathway of PI3K–Akt signaling pathway (KEGG: 04151). *The star element indicates *Z. officinale* targets associated with this pathway.

can accelerate tumor progression [84]. In this study, cellular response to cadmium is one of the top BPs (Supplementary Table S11).

Epithelial cell signaling in the *H. pylori* infection pathway (KEGG:05120) plays a key role in the development of gastric cancer. EGFR signaling in epithelial cells is essential for inflammation following *H. pylori* infection [76]. The *H. pylori* secretory protein HP0175 has been shown to bind toll-like receptor 4 (TLR4) and trigger EGFR transactivation in human gastric epithelial cells. This process is further associated with DNA damage through EGFR phosphorylation [76,85]. The *H. pylori* pathway is also connected to the PI3K/Akt signaling cascade, where the *H. pylori* cytotoxin-associated gene A (CagA) protein suppresses autophagy and promotes inflammation through activation of the c-Met–PI3K/Akt–mTOR pathway [86]. It is known that *H. pylori* transactivates the EGFR and predisposes to gastric cancer development in humans and animal models [87]. Notably, gingerol has been reported to exhibit anti-*H. pylori* activity [71]. Given the growing challenge of antibiotic overuse worldwide, which complicates the treatment of *H. pylori* infections [88], there is an increasing interest in exploring herbal medicines as promising alternative therapies [89,90]. Additionally, several studies have demonstrated that vitamins C and E can reduce *H. pylori* growth and neutrophil-driven inflammation [91].

The integrity of the tight junction is essential for maintaining the barrier function of epithelial cells. Disruption of these junctions, particularly in the intestine, can lead to a leaky gut associated with various gastrointestinal disorders [92]. This pathway involves bioactive compounds such as shogaols and alpha-tocopherol [69,73]. Studies have demonstrated that shogaols regulate tight junction-related proteins like claudin-2 and claudin-1 through the NF-κB signaling pathway, which helps keep the tight junctions intact and the barrier function of intestinal epithelial cells [73]. Alpha-tocopherol may also enhance the expression of tight junction proteins throughout the intestinal mucosa, thereby strengthening them and increasing transepithelial electrical resistance in intestinal cells [69].

AMPK is recognized for its role in modulating intestinal barrier integrity and controlling inflammation. Its

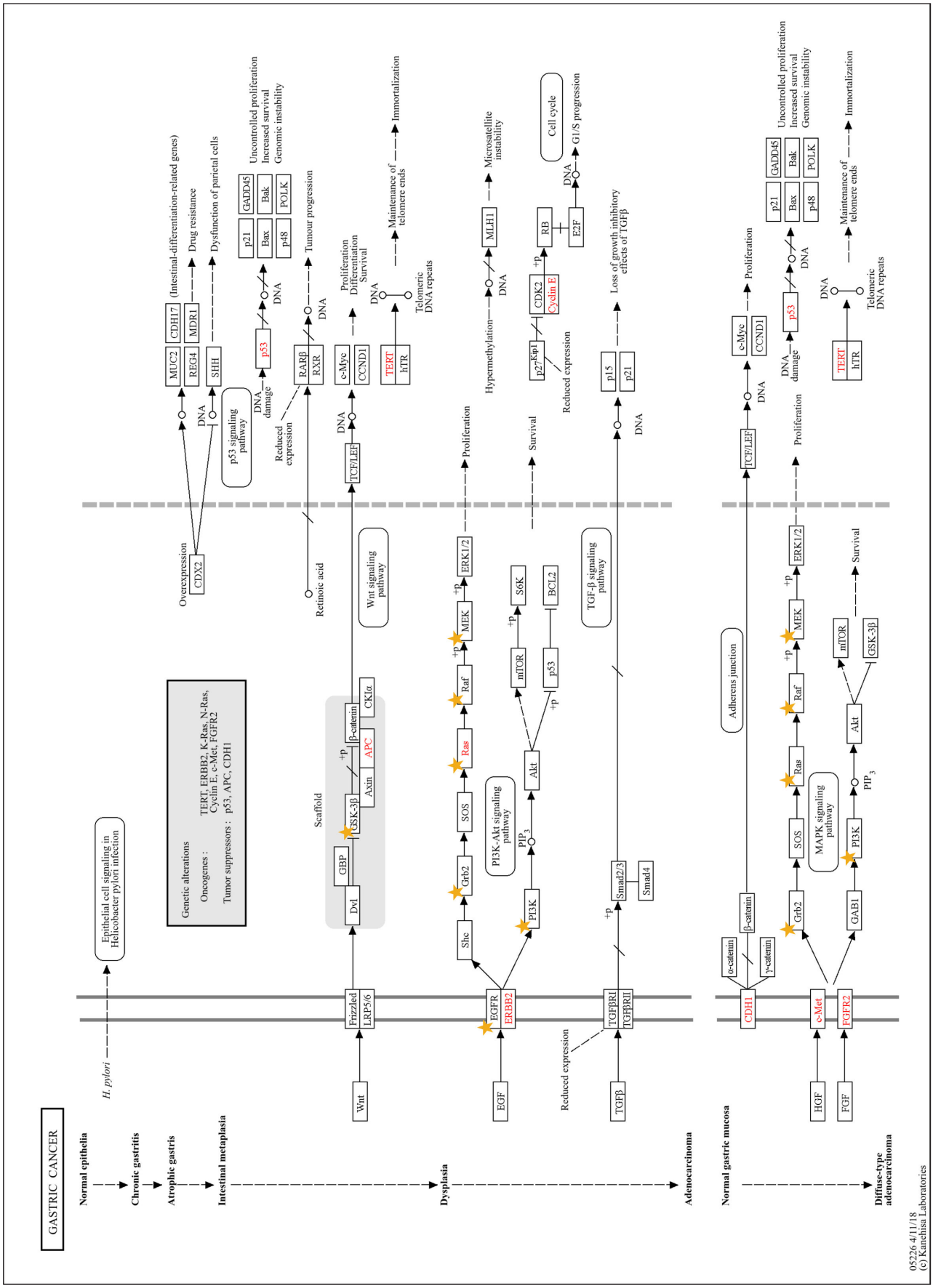

Figure 6. KEGG pathway of gastric cancer (KEGG:05226). *The star element indicates *Z. officinale* targets associated with this pathway. **The red genes indicate genetic alterations.

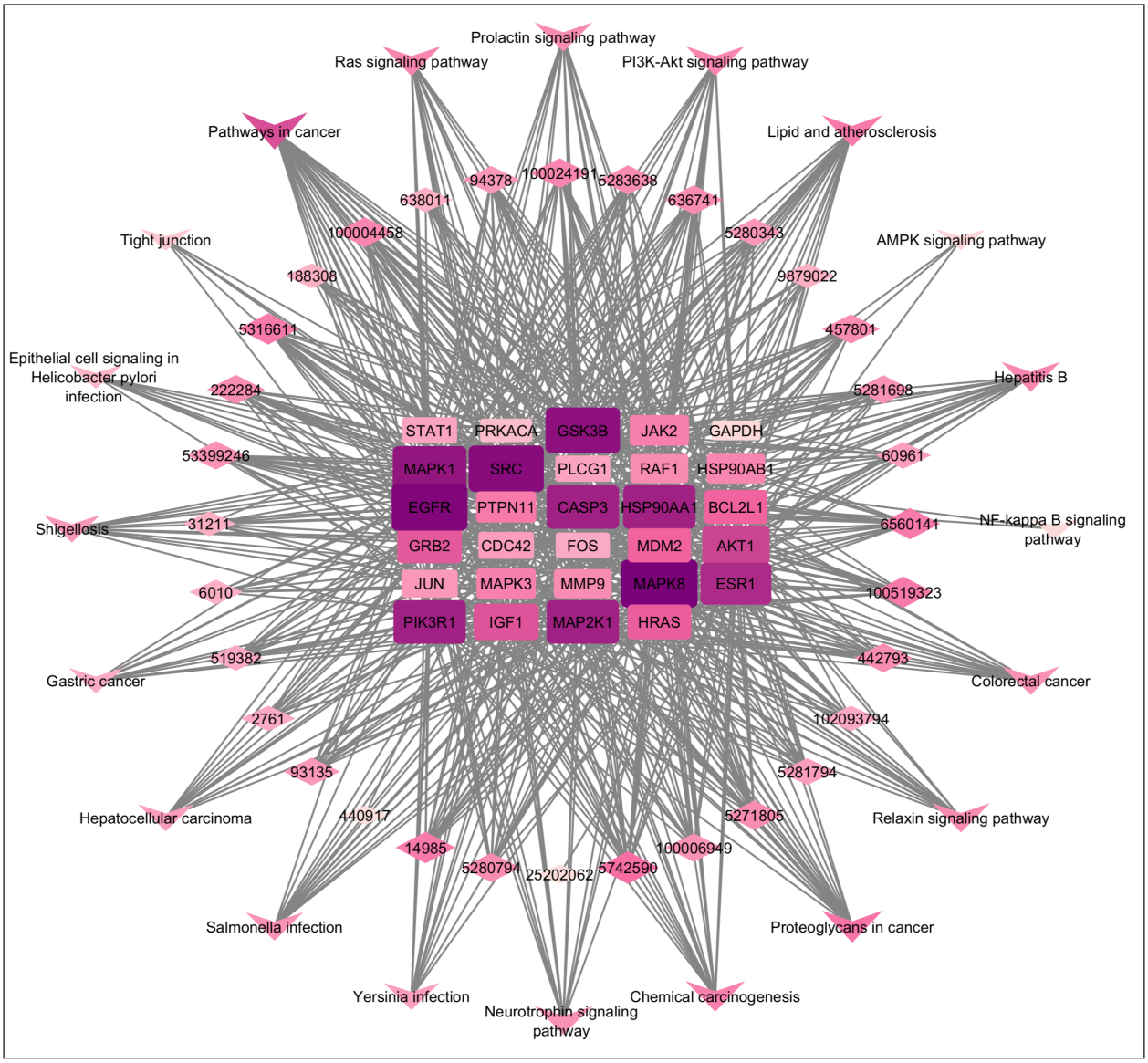

Figure 7. Construction of C-T-P network. V-shaped nodes represent the KEGG signaling pathways, diamond-shaped nodes represent the bioactive compounds, and rectangular nodes represent the crucial targets.

activation in intestinal epithelial cells is crucial for preserving barrier function and mitigating cytokine-induced damage. Research has demonstrated that treatment with 6-gingerol stimulates AMPK activation, leading to a reduction in colonic inflammatory cytokines, including IL-1β, IL-12, and TNF-α. This process has been shown to suppress NF-κB signaling and downregulate the expression of pro-inflammatory mediators such as TNF-α, inducible nitric oxide synthase, monocyte chemoattractant protein-1, cyclooxygenase-2, and matrix metalloproteinase-9 [93]. Additionally, phosphorylation of AMPK leads to the inhibition of phosphorylated target of rapamycin proteins activity, which in turn promotes autophagy. In FD, motility problems are linked to changes in interstitial cells of Cajal (ICC) and ghrelin. Ghrelin affects stomach movement through the mTOR pathway, and by activating AMPK, it can influence the motility issues in FD. However, disruption in ICC function may be related to altered autophagy, suggesting that the AMPK-mTOR pathway plays a role in the development of FD [4].

NF-κB is also involved in both gastric diseases and intestinal mucosal injury [94,95]. As a major transcriptional regulator, NF-κB controls genes involved in immune responses, cell growth, and genomic stability. It is essential for the host to defend against microbial infections and maintain intestinal barrier integrity. Moreover, *H. pylori*, which is a known risk factor for gastric cancer, can activate the NF-κB in gastric epithelial cells through pattern recognition receptors such as TLRs and NOD1, which detect bacterial components like CagA and peptidoglycan. This activation, mediated by the IKK complex, leads to NF-κB translocation into the nucleus,

where it triggers pro-inflammatory gene expression [96]. As previously mentioned, 6-shogaol was shown to inhibit TNF-α–induced activation of the NF-κB pathway in intestinal epithelial cells [78].

C-T-P network

We constructed the C-T-P network using Cytoscape software version 3.10.2, consisting of 29 crucial targets, 32 bioactive compounds, and 20 KEGG pathways. Figure 7 illustrates the C-T-P network's intricate interplay among crucial targets, bioactive compounds, and selected pathways. Rectangular nodes signify crucial targets, diamond-shaped nodes represent bioactive compounds in CID (Supplementary Table S2 for detailed information), and V-shaped nodes denote signaling pathways. Nodes with deeper shades (ranging from light pink to dark purple) and larger sizes signify higher DC values.

Molecular docking

Bioactive compounds with a higher DC, known for their relevance to gastrointestinal diseases, particularly in *Z. officinale*, such as gingerol and shogaol, were selected for molecular docking analysis. The chosen crucial compounds for docking included DDMHMH, alpha-tocopherol, gingerol, and shogaol. Thus, our investigation presents a new insight into the potential of this compound for future analysis, leading to its exclusion from further discussion and molecular docking analysis in this study. Additionally, crucial targets such as AKT1 and EGFR, exhibiting the highest DC, were chosen as the proteins for molecular docking analysis.

The results of the molecular docking analysis are presented in Table 1 (Supplementary Tables S13 and S14 for comprehensive details on binding energies and interaction profiles). Figure 8 provides 2D and 3D visualizations of the proteins and ligands involved in the study's molecular docking. The results revealed that among the tested bioactive compounds, DDMHMH exhibited satisfactory binding affinity towards both AKT1 and EGFR targets, with $\Delta G_{binding}$ values of −8.48 and −7.38 kcal/mol, respectively. DDMHMH also demonstrated favorable HADDOCK scores (−27.9 ± 5.7 for AKT1 and 16.6 ± 10.8 for EGFR) and substantial buried surface areas, indicating stable and potentially strong interactions. Although alpha-tocopherol showed a slightly stronger binding affinity than DDMHMH towards EGFR, DDMHMH was prioritized for further discussion due to its consistently strong interactions across both targets, AKT1 and EGFR, making it a more suitable candidate for subsequent MDS. In contrast, gingerol and shogaol exhibited relatively lower binding affinities, although their overall binding strengths remained within a favorable range.

Table 1. Molecular docking results.

Complex name	Binding affinity ΔG (kcal/mol) PRODIGY	HADDOCK score
AKT1–standard ligand	−8.71	−45.5 ± 2.9
AKT1–DDMHMH	−8.48	−27.9 ± 5.7
AKT1–alpha-tocopherol	−8.03	−27.5 ± 1.1
AKT1–gingerol	−6.38	−19.7 ± 0.4
AKT1–shogaol	−6.84	−15.4 ± 4.9
EGFR–standard ligand	−7.13	14.6 ± 13.3
EGFR–DDMHMH	−7.38	16.6 ± 10.8
EGFR–alpha-tocopherol	−7.49	23.4 ± 14.1
EGFR–gingerol	−7	11.6 ± 5.4
EGFR–shogaol	−6.76	29.0 ± 5.8

Molecular docking is used to predict the ability of molecules to bind to the target protein's binding site under static conditions [97]. The molecular docking results show a favorable change in Gibbs free energy (ΔG). Gibbs free energy measures the thermodynamic favorability of molecular interactions, with a lower or more negative ΔG indicating a stable and favorable binding interaction [58]. Protein−ligand binding occurs when ΔG is negative at equilibrium under constant pressure and temperature, like spontaneous processes [98]. Binding affinity thresholds provide insights into protein−ligand interaction strengths: a binding energy of <−4.25 kcal/mol indicates potential binding, <−5.00 kcal/mol indicates good binding strength, and <−7.00 kcal/mol signifies satisfactory binding strength [99]. Molecular docking results show that the EGFR–shogaol, AKT1–gingerol, and AKT1–shogaol complexes demonstrated good binding affinity (<−5.00 kcal/mol), while the remaining complexes, DDMHMH and alpha-tocopherol, with both EGFR and AKT1, exhibited satisfactory binding affinity (<−7.00 kcal/mol).

Molecular dynamics simulation

The MDS analysis provided in Figure 9 comprehensively compares the dynamic behavior of AKT1 protein complexes with DDMHMH (top-performing ligand) and MK−2206 (a known standard inhibitor of AKT1), assessed over a 50^{-ns} simulation period. In Figure 9A, the root mean square deviation (RMSD) plot indicates that the AKT1−DDMHMH complex exhibits greater structural stability throughout the trajectory, maintaining a lower average RMSD value of approximately 0.780 nm. In contrast, the AKT1−MK−2206 complex demonstrates significant conformational fluctuations, reaching an average RMSD of 1.415 nm with sharp deviations particularly in the early phase (10–20 ns), suggesting that the binding of MK−2206 may induce more structural rearrangements and less conformational stability. Figure 9B illustrates the root mean square fluctuation (RMSF), which reflects the flexibility of individual amino acid residues throughout the simulation. Both AKT1 complexes, bound to DDMHMH and MK−2206, exhibited a comparable fluctuation profile, with a prominent spike observed between residues Trp80 and Phe150. This region likely corresponds to an active or regulatory loop critical for receptor function. The observed spike suggests increased local mobility, which may disrupt hydrogen bonding networks within this domain and interfere with receptor signaling. DDMHMH induces a similar disruption pattern to MK−2206 (an established allosteric AKT1 inhibitor), implying that DDMHMH may exert an antagonistic

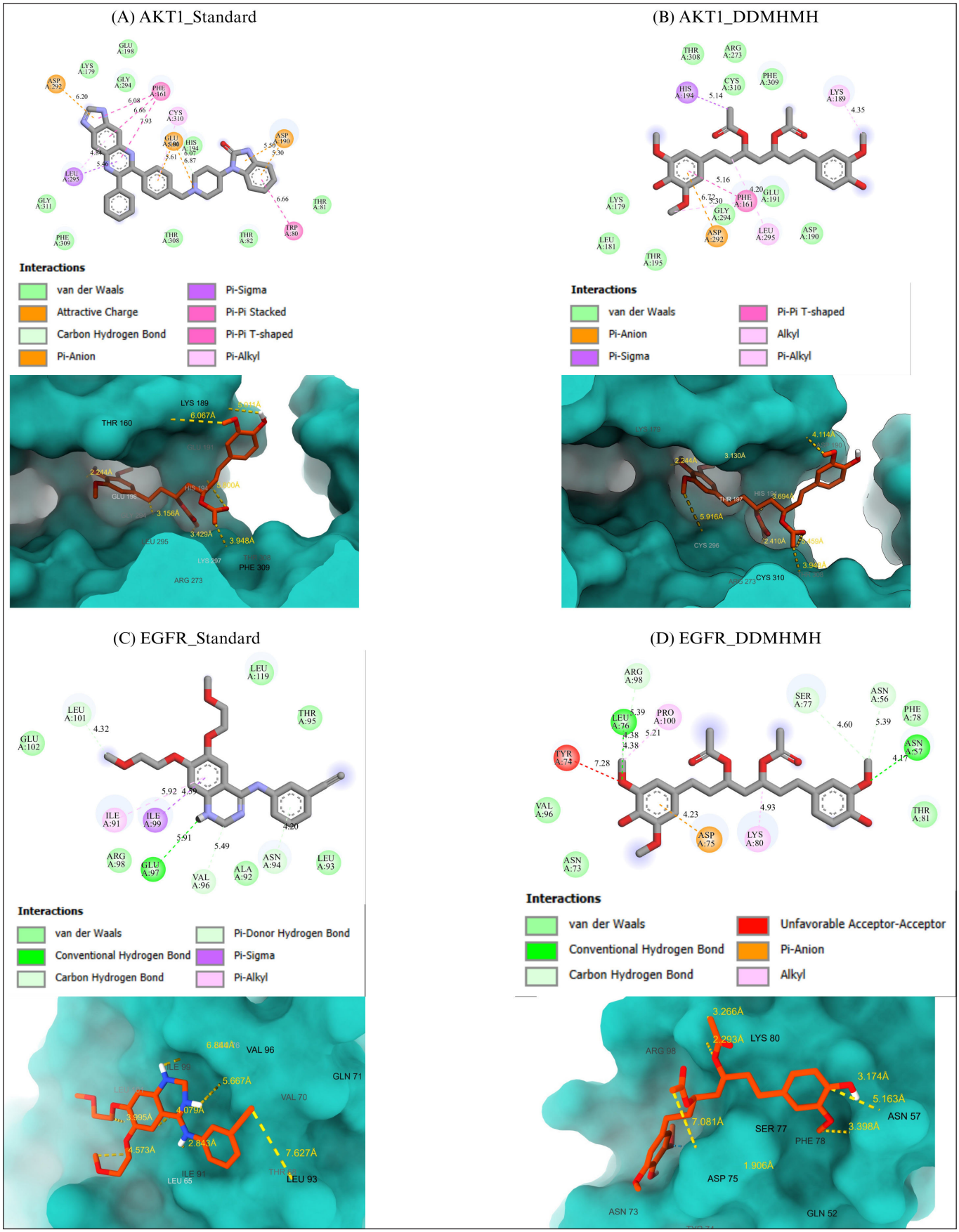

Figure 8. 2D and 3D molecular docking diagrams of the bioactive compounds within *Z. officinale* and targets linked to dyspepsia. (A) AKT1–Standard. (B) AKT1–DDMHMH. (C) EGFR–Standard. (D) EGFR–DDMHMH.

effect. By altering the dynamic behavior of key regulatory residues, DDMHMH could impair the conformational integrity required for AKT1 activation, thereby mimicking the inhibitory mechanism of MK−2206. This functional mimicry reinforces DDMHMH's potential as a viable AKT1 antagonist.

In terms of compactness, the radius of gyration (RoG) results shown in Figure 9C demonstrate that both complexes retained consistent structural compactness throughout the simulation. However, the AKT1−DDMHMH complex maintained slightly lower RoG values, particularly in the latter part of the simulation (after 35 ns), which may suggest a more tightly packed protein−ligand complex. This tighter packing could be attributed to better accommodation of DDMHMH within the AKT1 binding pocket, potentially contributing to enhanced structural integrity and favorable intramolecular interactions. Hydrogen bonding interactions, which are critical indicators of binding affinity and stability, are presented in Figure 9D. Throughout the simulation, the AKT1−DDMHMH complex consistently exhibited a slightly higher number of intermolecular hydrogen bonds compared to the AKT1−MK−2206 complex. While both ligands formed between 0 and 5 hydrogen bonds at various points, DDMHMH demonstrated more frequent and persistent hydrogen bond interactions, which likely contribute to its more stable RMSD and compact structure. This observation further supports the notion that DDMHMH forms more stable and favorable interactions within the binding site of AKT1.

Moving to the EGFR complexes, the RMSD plot (Fig. 10A) tracks the structural deviation of the protein−ligand complex over time, serving as a proxy for overall stability.

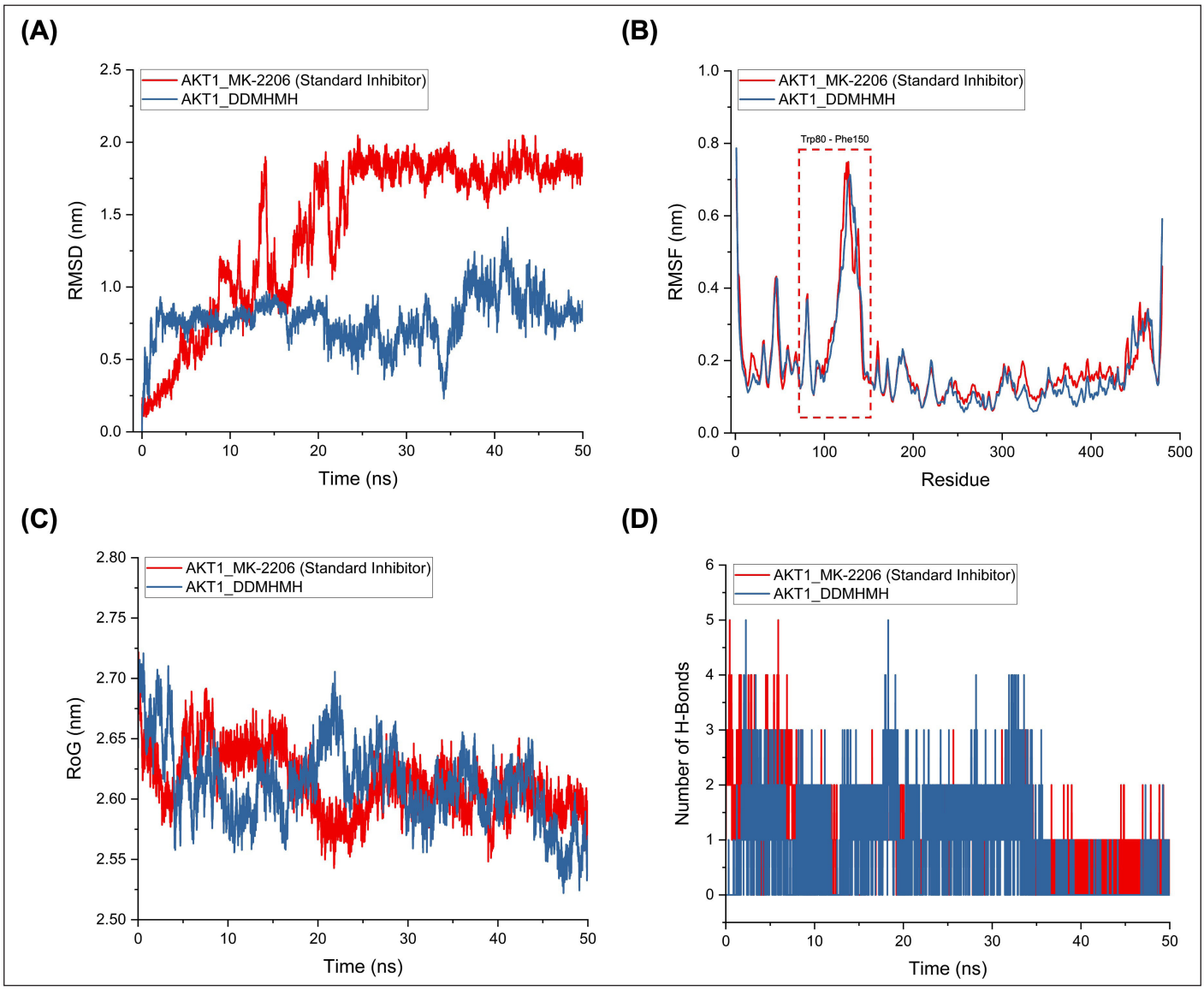

Figure 9. MDS were conducted to evaluate the stability and interactions of AKT1-ligand complexes, comparing DDMHMH (the top-performing ligand) with MK−2206 (the standard inhibitor). (A) RMSD to assess overall structural stability. (B) RMSF to examine residue-level flexibility. (C) RoG to evaluate structural compactness. (D) The hydrogen bond (H−bond) count is used to characterize intermolecular interactions.

EGFR complexed with DDMHMH demonstrated a more stable trajectory, with an average RMSD of 10.483 nm, compared to 10.952 nm for the EGFR−Erlotinib (standard inhibitor) complex. While both values are relatively high when compared to previously reported AKT1−ligand complexes (ranging from 0.780 to 1.415 nm), the lower RMSD value of DDMHMH indicates improved conformational consistency during the simulation. However, the abnormally high RMSD values observed here for EGFR are likely attributed to structural characteristics such as extended loops or disordered terminal regions, which may have caused large coordinate shifts without compromising the local stability of the ligand-binding region. This elevation in RMSD does not necessarily reflect true instability of the protein-ligand complex but may be influenced by technical aspects of the simulation setup, including initial model configuration. Furthermore, the use of the CHARMM27 force field, while reliable for protein simulations, may exhibit variability when applied to large or highly flexible proteins such as EGFR.

Figure 10B examines the RMSF values, reflecting the flexibility of individual amino acid residues throughout the simulation. Both ligands produced generally similar RMSF profiles across the EGFR backbone, suggesting that neither compound induced abnormal local flexibility or instability. However, a pronounced fluctuation was detected within the Leu90–Asn110 residue region, denoted with a red dashed box. This region may represent a flexible loop or surface-exposed region affected by ligand binding. Interestingly, DDMHMH

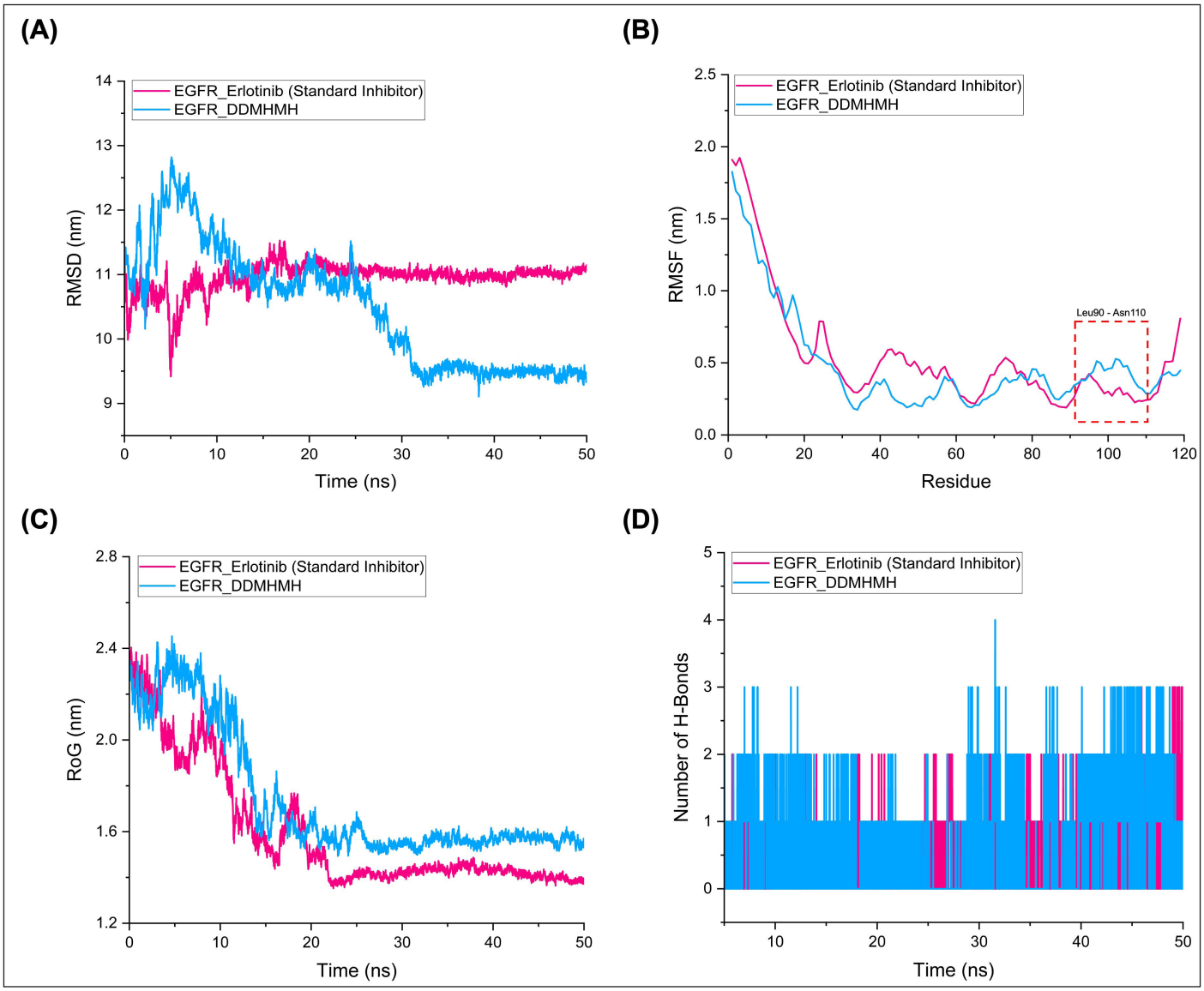

Figure 10. Dynamic simulation analysis was employed to explore the behavior of EGFR in complex ligands, comparing the top-performing ligand (DDMHMH) with the benchmark Erlotinib (standard inhibitor). The evaluation included: (A) Tracking RMSD values to monitor conformational consistency over time, (B) Analyzing RMSF to reveal flexibility patterns across amino acid residues, (C) Measuring the RoG to gauge the degree of molecular compactness, and (D) Quantifying H−bond events to understand the strength and stability of ligand–receptor interactions.

displayed slightly reduced residue fluctuation in this region compared to Erlotinib, which could suggest tighter anchoring or more restrained interactions at this segment. The preservation of backbone flexibility, especially in non-core residues, can be beneficial for maintaining necessary protein functions while allowing selective inhibition.

The RoG plot (Fig. 10C) provides insight into the compactness and overall folding behavior of the protein−ligand complex. The average RoG for EGFR−DDMHMH was calculated at 1.740 nm, whereas the EGFR−Erlotinib was lower at 1.594 nm. This suggests that the EGFR structure is slightly more expanded when bound to DDMHMH, which may reflect either a looser packing or conformational adaptation of the binding pocket to accommodate the ligand. Despite the reduced compactness, the RoG values stabilized after ~25 ns in both cases, indicating that the systems reached a dynamic equilibrium. A less compact structure is not necessarily disadvantageous; in some cases, it might enhance accessibility of residues to solvent or improve flexibility in regulatory regions. Figure 10D illustrates the temporal distribution of hydrogen bonds between EGFR and the ligands. Hydrogen bonding plays a pivotal role in ligand binding affinity and specificity. DDMHMH consistently maintained a higher average number of hydrogen bonds compared to Erlotinib, often forming 2–4 H−bonds throughout the simulation, whereas Erlotinib interactions fluctuated more and generally formed fewer H−bonds. This pattern indicates that DDMHMH forms stronger and more persistent polar interactions with the EGFR binding pocket, which can contribute to improved binding affinity and stability. Moreover, the presence of frequent hydrogen bond peaks suggests that DDMHMH may form dynamic interactions with multiple residues, enhancing binding versatility. Despite the elevated RMSD, supporting parameters such as RoG, hydrogen bonding analysis, and RMSF profiles suggest that the EGFR–DDMHMH complex maintained favorable and stable interactions throughout the simulation.

MM/PBSA calculations

The binding free energy ($\Delta G_{binding}$) values obtained from MM/PBSA calculations (Table 2) provide quantitative insights into the ligand–protein interaction strength for both AKT1 and EGFR complexes. For AKT1, the reference inhibitor MK−2206 demonstrated a significantly more favorable binding energy (−21.53 ± 4.98 kcal/mol) compared to DDMHMH (−8.71 ± 1.57 kcal/mol), suggesting that while DDMHMH interacts with AKT1, it does so with considerably lower binding affinity. Although DDMHMH showed a weaker binding to AKT1 compared to MK−2206 (−8.71 *vs.* −21.53 kcal/mol), the compound induced similar residue fluctuations in critical regions, particularly Trp80–Phe150, indicating potential interaction through hydrogen bond disruption. However, the relatively modest binding free energy toward AKT1 suggests that DDMHMH may not act as a strong AKT1 inhibitor. In contrast, the EGFR−DDMHMH complex exhibited a more favorable binding free energy (−11.44 ± 1.80 kcal/mol) than the EGFR−Erlotinib complex (−7.58 ± 8.63 kcal/mol), indicating that DDMHMH may exhibit a more stable and stronger binding to EGFR than the clinically approved Erlotinib. The lower standard deviation in DDMHMH's binding to EGFR further supports the consistency and reliability of this interaction. These findings suggest that although DDMHMH is less effective than MK−2206 in targeting AKT1, it shows promising potential as an EGFR inhibitor, possibly through stable hydrogen bonding and favorable conformational compatibility within the EGFR binding pocket. Although molecular docking results indicated that DDMHMH exhibited a slightly stronger binding affinity to EGFR (−7.36 kcal/mol) compared to Erlotinib (−7.13 kcal/mol), the MM/PBSA binding free energy analysis revealed a more favorable binding for DDMHMH (−11.44 *vs.* −7.58 kcal/mol). This apparent discrepancy arises from the fundamental differences between the two approaches: docking provides a static, rigid-body approximation of binding based on a single conformation, whereas MM/PBSA incorporates dynamic structural and energetic information over time from MDS. The improved MM/PBSA score for DDMHMH suggests that, despite an initially modest docking score, the ligand forms more stable and favorable interactions with EGFR under physiologically relevant, flexible conditions, highlighting its potential as a more effective binder during dynamic protein–ligand association.

Table 2. Binding free energy ($\Delta G_{binding}$) results from MM/PBSA calculations for the AKT1 and EGFR complexes are reported as mean values accompanied by standard deviations, expressed in kcal/mol.

Complex	MM/PBSA calculation results $\Delta G_{binding}$ (kcal/mol)
AKT1–MK-2206	−21.53 ± 6.94
AKT1–DDMHMH	−8.71 ± 6.49
EGFR– Erlotinib	−7.58 ± 1.65
EGFR–DDMHMH	−11.44 ± 2.82

CONCLUSION

This study provides a comprehensive analysis of the potential therapeutic mechanisms by which *Z. officinale* may alleviate dyspepsia symptoms, integrating network pharmacology, molecular docking, MDS, and binding free energy calculations. Through the C−T−P network, key bioactive compounds such as DDMHMH, alpha−tocopherol, gingerol, and shogaol were identified, with AKT1 and EGFR emerging as central therapeutic targets. KEGG pathway enrichment highlighted their involvement in dyspepsia-related signaling pathways, including PI3K−Akt, gastric cancer, epithelial cell signaling in *H. pylori* infection, the tight junction, AMPK, and NF-κB signaling. Molecular docking revealed favorable interactions, especially between DDMHMH and both AKT1 and EGFR ($\Delta G_{binding}$ scores <−7.00 kcal/mol). Notably, MDS showed that DDMHMH maintained stable binding with EGFR, demonstrated by consistent RMSD, higher hydrogen bonding, and stronger MM/PBSA binding energy (−11.44 ± 2.82 kcal/mol) than the standard ligand, Erlotinib.

However, this study has several limitations. As this research relies solely on *in silico* methods, including network pharmacology, molecular docking, and dynamics simulation, the results are preliminary and should be supported by subsequent pharmacological and molecular biology experiments to confirm

their biological significance. The bioactive compounds are selected based on computational network metrics such as DC, without consideration of their actual concentrations in *Z. officinale*. For example, DDMHMH's natural abundance remains unquantified or very low, and the inclusion of alpha-tocopherol, which is not the primary constituent of ginger, may limit the specificity of the results. Nevertheless, this finding leads to the identification of less-studied molecular targets and interactions, highlighting potential new directions for future research. Further *in vitro* and *in vivo* validation is recommended to support the therapeutic potential of *Z. officinale* in dyspepsia treatment.

ACKNOWLEDGMENT

We would like to thank Dexa Medica for their support and resources provided during this study.

AUTHOR CONTRIBUTIONS

All authors made substantial contributions to conception and design, acquisition of data, or analysis and interpretation of data; took part in drafting the article or revising it critically for important intellectual content; agreed to submit to the current journal; gave final approval of the version to be published; and agree to be accountable for all aspects of the work. All the authors are eligible to be an author as per the International Committee of Medical Journal Editors (ICMJE) requirements/guidelines.

FINANCIAL SUPPORT

This study was financially supported by Dexa Medica.

CONFLICT OF INTEREST

The authors report no financial or any other conflicts of interest in this work.

CONSENT TO PARTICIPATE

Not applicable, as this study does not involve human participants.

ETHICAL APPROVAL

This study does not involve experiments on animals or human subjects.

DATA AVAILABILITY

All relevant data generated or analyzed during this study are included in the supplementary tables and figures provided with this article.

PUBLISHER'S NOTE

All claims expressed in this article are solely those of the authors and do not necessarily represent those of the publisher, the editors and the reviewers. This journal remains neutral with regard to jurisdictional claims in published institutional affiliation.

USE OF ARTIFICIAL INTELLIGENCE (AI)-ASSISTED TECHNOLOGY

The authors declares that they have not used artificial intelligence (AI)-tools for writing and editing of the manuscript, and no images were manipulated using AI.

REFERENCES

1. Moayyedi PM, Lacy BE, Andrews CN, Enns RA, Howden CW, Vakil N. ACG and CAG clinical guideline: management of dyspepsia. Am J Gastroenterol. 2017;112(7):988–1013. doi: https://doi.org/10.1038/ajg.2017.154
2. Oustamanolakis P, Tack J. Dyspepsia: organic versus functional. J Clin Gastroenterol. 2012;46(3):175–90. doi: https://doi.org/10.1097/MCG.0b013e318241b335
3. Tjandrawinata RR, Nailufar F, Arifin PF. Hydrogen potassium adenosine triphosphatase activity inhibition and downregulation of its expression by bioactive fraction DLBS2411 from *Cinnamomum burmannii* in gastric parietal cells. Int J Gen Med. 2013;6:807–15. doi: https://doi.org/10.2147/IJGM.S50134
4. Song Y, Yin D, Zhang Z, Chi L. Research progress of treatment of functional dyspepsia with traditional Chinese medicine compound based on cell signal pathway. Front Pharmacol. 2023;13:1–9. doi: https://doi.org/10.3389/fphar.2022.1089231
5. Kang SJ, Park B, Shin CM. *Helicobacter pylori* eradication therapy for functional dyspepsia: a meta-analysis by region and *H. pylori* prevalence. J Clin Med. 2019;8(9):1–18. doi: https://doi.org/10.3390/jcm8091324
6. Gwee K, Holtmann G, Tack J, Suzuki H, Liu J, Xiao Y, *et al.* Herbal medicines in functional dyspepsia—untapped opportunities not without risks. Neurogastroenterol Motil. 2021;33(2):1–13. doi: https://doi.org/10.1111/nmo.14044
7. Wang C, Huanbieke N, Cai X, Gao S, Du T, Zhou Z, *et al.* Integrating network pharmacology and *in vivo* model to investigate the mechanism of Biheimaer in the treatment of functional dyspepsia. eCAM. 2022;2022:1–13. doi: https://doi.org/10.1155/2022/8773527
8. Schulz RM, Ahuja NK, Slavin JL. Effectiveness of nutritional ingredients on upper gastrointestinal conditions and symptoms: a narrative review. Nutrients. 2022;14(3):1–23. doi: https://doi.org/10.3390/nu14030672
9. Nailufar F, Tjandrawinata RR. The evaluation of proton pump inhibitor bioactive fraction DLBS2411 from *Cinnamomum burmannii* (Nees & T. Nees) in animal model of gastric ulceration healing. AJPT. 2018;12(4):79–88. doi: https://doi.org/10.3844/ajptsp.2017.79.88
10. Tjandrawinata R, Nailufar F. Gastroprotective effect of DLBS2411 bioactive fraction from *Cinnamomum burmannii* against ethanol-induced gastric damage in rats. J Exp Pharmacol. 2020;12:87–95. doi: https://doi.org/10.2147/JEP.S244223
11. Salea R, Veriansyah B, Tjandrawinata RR. Optimization and scale-up process for supercritical fluids extraction of ginger oil from *Zingiber officinale* var. Amarum. J Supercrit Fluids. 2017;120:285–94. doi: https://doi.org/10.1016/j.supflu.2016.05.035
12. Aregawi LG, Zoltan C. Evaluation of adverse effects and tolerability of dietary ginger supplementation in patients with functional dyspepsia. Curr Ther Res. 2025;102:1–5. doi: https://doi.org/10.1016/j.curtheres.2025.100792
13. Wulandari AS, Tandrasasmita OM, Tjandrawinata RR. Bioactive fraction dlbs2411 from *Cinnamomum burmannii*, (Nees and t. nees) blume as colon and gastroprotector by stimulating muc5ac and cyclooxygenase-2 gene expression. IJPPS. 2016;8(8):202–7.
14. Haniadka R, Saldanha E, Sunita V, Palatty PL, Fayad R, Baliga MS. A review of the gastroprotective effects of ginger (*Zingiber officinale* Roscoe). Food Funct. 2013;4(6):845–55. doi: https://doi.org/10.1039/c3fo30337c
15. Lete I, Allué J. The effectiveness of ginger in the prevention of nausea and vomiting during pregnancy and chemotherapy. Integr Med. 2016;11:11–7. doi: https://doi.org/10.4137/IMI.S36273
16. Aregawi LG, Shokrolahi M, Gebremeskel TG, Zoltan C. The effect of ginger supplementation on the improvement of dyspeptic symptoms in patients with functional dyspepsia. Cureus. 2023;15(9):1–8. doi: https://doi.org/10.7759/cureus.46061
17. Li L, Yang L, Yang L, He C, He Y, Chen L, *et al.* Network pharmacology: a bright guiding light on the way to explore the

personalized precise medication of traditional Chinese medicine. Chin Med. 2023;18(1):1–19. doi: https://doi.org/10.1186/s13020-023-00853-2
18. Tjandrawinata RR, Amalia AW, Tuna H, Said VN, Tan S. Molecular mechanisms of network pharmacology-based immunomodulation of Huangqi (*Astragali radix*). JIFI. 2022;20(2):184–95. doi: https://doi.org/10.35814/jifi.v20i2.1301
19. Tan S, Tjandrawinata R, Prasasty V. Molecular mechanism of DLBS3233 bioactive fraction in type-2 diabetes mellitus: network pharmacology and docking study. Sains Malays. 2023;52(12):3497–800. doi: https://doi.org/10.17576/jsm-2023-5212-12
20. Tan S, Yulandi A, Tjandrawinata RR. Network pharmacology study of *Phyllanthus niruri*: potential target proteins and their hepatoprotective activities. J App Pharm Sci. 2023;13(12):232–42. doi: https://doi.org/10.7324/JAPS.2023.146937
21. Gunathilake K, Rupasinghe HV. Recent perspectives on the medicinal potential of ginger. BTAT. 2015;5:55–63. doi: https://doi.org/10.2147/BTAT.S68099
22. Sharma S, Shukla MK, Sharma KC, Tirath, Kumar L, Anal JMH, *et al.* Revisiting the therapeutic potential of gingerols against different pharmacological activities. Naunyn Schmiedebergs Arch Pharmacol. 2023;396(4):633–47. doi: https://doi.org/10.1007/s00210-022-02372-7
23. Kong X, Liu C, Zhang Z, Cheng M, Mei Z, Li X, *et al.* BATMAN-TCM 2.0: an enhanced integrative database for known and predicted interactions between traditional Chinese medicine ingredients and target proteins. Nucleic Acids Res. 2024;52(D1):1110–20. doi: https://doi.org/10.1093/nar/gkad926
24. Ru J, Li P, Wang J, Zhou W, Li B, Huang C, *et al.* TCMSP: a database of systems pharmacology for drug discovery from herbal medicines. J Cheminf. 2014;6(1):1–6. doi: https://doi.org/10.1186/1758-2946-6-13
25. Lv X, Xu Z, Xu G, Li H, Wang C, Chen J, *et al.* Investigation of the active components and mechanisms of *Schisandra chinensis* in the treatment of asthma based on a network pharmacology approach and experimental validation. Food Funct. 2020;11(4):3032–42. doi: https://doi.org/10.1039/D0FO00087F
26. Daina A, Michielin O, Zoete V. SwissADME: a free web tool to evaluate pharmacokinetics, drug-likeness and medicinal chemistry friendliness of small molecules. Sci Rep. 2017;7(1):1–13. doi: https://doi.org/10.1038/srep42717
27. Abagyan R, Totrov M, Kuznetsov D. ICM—a new method for protein modeling and design: applications to docking and structure prediction from the distorted native conformation. J Comput Chem. 1994;15(5):488–506. doi: https://doi.org/10.1002/jcc.540150503
28. Kim S, Chen J, Cheng T, Gindulyte A, He J, He S, *et al.* PubChem 2023 update. Nucleic Acids Res. 2023;51(D1):1373–80. doi: https://doi.org/10.1093/nar/gkac956
29. Keiser MJ, Roth BL, Armbruster BN, Ernsberger P, Irwin JJ, Shoichet BK. Relating protein pharmacology by ligand chemistry. Nat Biotechnol. 2007;25(2):197–206. doi: https://doi.org/10.1038/nbt1284
30. Xia W, Yihang S, Shiwei W, Shiliang L, Weilin Z, Xiaofeng L, *et al.* PharmMapper 2017 update: a eeb server for potential drug target identification with a comprehensive target pharmacophore database. Nucleic Acids Res. 2017;45(W1):356–60. doi: https://doi.org/10.1093/nar/gkx374
31. Wang X, Pan C, Gong J, Liu X, Li H. Enhancing the enrichment of pharmacophore-based target prediction for the polypharmacological profiles of drugs. J Chem Inf Model. 2016;56(6):1175–83. doi: https://doi.org/10.1021/acs.jcim.5b00690
32. Burley SK, Bhikadiya C, Bi C, Bittrich S, Chao H, Chen L, *et al.* RCSB protein data bank (RCSB.org): delivery of experimentally-determined PDB structures alongside one million computed structure models of proteins from Artificial Intelligence/Machine Learning. Nucleic Acids Res. 2023;51(D1):488–508. doi: https://doi.org/10.1093/nar/gkac1077
33. The UniProt Consortium. UniProt: the universal protein knowledgebase in 2023. Nucleic Acids Res. 2023;51(D1):523–31. doi: https://doi.org/10.1093/nar/gkac1052
34. Bardou P, Mariette J, Escudié F, Djemiel C, Klopp C. jvenn: an interactive venn diagram viewer. BMC Bioinform. 2014;15(1):1–7. doi: https://doi.org/10.1186/1471-2105-15-293
35. Stelzer G, Rosen N, Plaschkes I, Zimmerman S, Twik M, Fishilevich S, *et al.* The GeneCards suite: from gene data mining to disease genome sequence analyses. Curr Protoc Bioinform. 2016;54(1):1–33. doi: https://doi.org/10.1002/cpbi.5
36. Piñero J, Ramírez-Anguita JM, Saüch-Pitarch J, Ronzano F, Centeno E, Sanz F, *et al.* The DisGeNET knowledge platform for disease genomics: 2019 update. Nucleic Acids Res. 2020;48(D1):845–55. doi: https://doi.org/10.1093/nar/gkz1021
37. Sayers EW, Beck J, Bolton EE, Brister JR, Chan J, Comeau DC, *et al.* Database resources of the national center for biotechnology information. Nucleic Acids Res. 2024;52(D1):33–43. doi: https://doi.org/10.1093/nar/gkad1044
38. Doncheva NT, Morris JH, Gorodkin J, Jensen LJ. Cytoscape StringApp: network analysis and visualization of proteomics data. J Proteome Res. 2019;18(2):623–32. doi: https://doi.org/10.1021/acs.jproteome.8b00702
39. Shannon P, Markiel A, Ozier O, Baliga NS, Wang JT, Ramage D, *et al.* Cytoscape: a software environment for integrated models of biomolecular interaction networks. Genome Res. 2003;13(11):2498–504. doi: https://doi.org/10.1101/gr.1239303
40. Tang Y, Li M, Wang J, Pan Y, Wu F-X. CytoNCA: a cytoscape plugin for centrality analysis and evaluation of protein interaction networks. Biosystems. 2014;127:67–72. doi: https://doi.org/10.1016/j.biosystems.2014.11.005
41. Li F, Duan J, Zhao M, Huang S, Mu F, Su J, *et al.* A network pharmacology approach to reveal the protective mechanism of *Salvia miltiorrhiza-Dalbergia odorifera* coupled-herbs on coronary heart disease. Sci Rep. 2019;9(1):1–12. doi: https://doi.org/10.1038/s41598-019-56050-5
42. Kuleshov MV, Jones MR, Rouillard AD, Fernandez NF, Duan Q, Wang Z, *et al.* Enrichr: a comprehensive gene set enrichment analysis web server 2016 update. Nucleic Acids Res. 2016;44(Web Server issue):90–7. doi: https://doi.org/10.1093/nar/gkw377
43. Aleksander SA, Balhoff J, Carbon S, Cherry JM, Drabkin HJ, Ebert D, *et al.* The gene ontology knowledgebase in 2023. Genetics. 2023;224(1):1–14. doi: https://doi.org/10.1093/genetics/iyad031
44. Kanehisa M, Furumichi M, Sato Y, Kawashima M, Ishiguro-Watanabe M. KEGG for taxonomy-based analysis of pathways and genomes. Nucleic Acids Res. 2023;51(D1):587–92. doi: https://doi.org/10.1093/nar/gkac963
45. Tang D, Chen M, Huang X, Zhang G, Zeng L, Zhang G, *et al.* SRplot: a free online platform for data visualization and graphing. PLoS One. 2023;18(11):1–18. doi: https://doi.org/10.1371/journal.pone.0294236
46. Shang L, Wang Y, Li J, Zhou F, Xiao K, Liu Y, *et al.* Mechanism of Sijunzi decoction in the treatment of colorectal cancer based on network pharmacology and experimental validation. J Ethnopharmacol. 2023;302:1–19. doi: https://doi.org/10.1016/j.jep.2022.115876
47. Wang F, Chen J-H, Liu B, Zhang T. Analysis of the active components and mechanism of three prescriptions in the treatment of COVID-19 via network pharmacology and molecular docking. Nat Prod Commun. 2021;16(9):1–12. doi: https://doi.org/10.1177/1934578X211047702
48. de Vries SJ, van Dijk M, Bonvin AMJJ. The HADDOCK web server for data-driven biomolecular docking. Nat Protoc. 2010;5(5):883–97. doi: https://doi.org/10.1038/nprot.2010.32
49. Stamos J, Sliwkowski MX, Eigenbrot C. Structure of the epidermal growth factor receptor kinase domain alone and in complex with a 4-anilinoquinazoline inhibitor *. J Biol Chem. 2002;277(48):46265–72. doi: https://doi.org/10.1074/jbc.M207135200

50. BIOVIA, Dassault Systèmes. BIOVIA discovery studio modeling environment, version 24.1.0.23298. San Diego, CA: Dassault Systèmes; 2023.
51. Varadi M, Bertoni D, Magana P, Paramval U, Pidruchna I, Radhakrishnan M, *et al.* AlphaFold protein structure database in 2024: providing structure coverage for over 214 million protein sequences. Nucleic Acids Res. 2024;52(D1):368–75. doi: https://doi.org/10.1093/nar/gkad1011
52. Ye B, Tian W, Wang B, Liang J. CASTpFold: computed atlas of surface topography of the universe of protein folds. Nucleic Acids Res. 2024;52(W1):194–9. doi: https://doi.org/10.1093/nar/gkae415
53. Alotaiq N, Dermawan D. Computational investigation of montelukast and its structural derivatives for binding affinity to dopaminergic and serotonergic receptors: insights from a comprehensive molecular simulation. Pharmaceuticals. 2025;18(4):1–36. doi: https://doi.org/10.3390/ph18040559
54. Khan MN, Farooq U, Khushal A, Wani TA, Zargar S, Khan S. Unraveling potential EGFR kinase inhibitors: computational screening, molecular dynamics insights, and MMPBSA analysis for targeted cancer therapy development. PLoS One. 2025;20(5):1–23. doi: https://doi.org/10.1371/journal.pone.0321500
55. Xing Y, Lin NU, Maurer MA, Chen H, Mahvash A, Sahin A, *et al.* Phase II trial of AKT inhibitor MK-2206 in patients with advanced breast cancer who have tumors with PIK3CA or AKT mutations, and/or PTEN loss/PTEN mutation. BCR. 2019;21(1):1–12. doi: https://doi.org/10.1186/s13058-019-1154-8
56. Laskowski RA, Jabłońska J, Pravda L, Vařeková RS, Thornton JM. PDBsum: structural summaries of PDB entries. Protein Sci. 2018;27(1):129–34. doi: https://doi.org/10.1002/pro.3289
57. Vangone A, Schaarschmidt J, Koukos P, Geng C, Citro N, Trellet ME, *et al.* Large-Scale prediction of binding affinity in protein–small ligand complexes: the PRODIGY-LIG web server. Bioinformatics. 2019;35(9):1585–7. doi: https://doi.org/10.1093/bioinformatics/bty816
58. Syahbanu F, Giriwono PE, Tjandrawinata RR, Suhartono MT. Molecular docking of subtilisin K2, a fibrin-degrading enzyme from Indonesian Moromi, with its substrates. Food Sci Technol. 2021;42:1–8. doi: https://doi.org/10.1590/fst.61820
59. Meng EC, Goddard TD, Pettersen EF, Couch GS, Pearson ZJ, Morris JH, *et al.* UCSF ChimeraX: tools for structure building and analysis. Protein Sci. 2023;32(11):1–13. doi: https://doi.org/10.1002/pro.4792
60. Abraham M, Alekseenko A, Basov V, Bergh C, Briand E, Brown A, *et al.* GROMACS 2024.3 Manual. 2024. Available from: https://zenodo.org/records/13457083. doi: https://doi.org/10.5281/zenodo.13457083
61. Valdés-Tresanco MS, Valdés-Tresanco ME, Valiente PA, Moreno E. gmx_MMPBSA: a new tool to perform end-state free energy calculations with GROMACS. J Chem Theory Comput. 2021;17(10):6281–91. doi: https://doi.org/10.1021/acs.jctc.1c00645
62. Guo W, Huang J, Wang N, Tan H-Y, Cheung F, Chen F, *et al.* Integrating network pharmacology and pharmacological evaluation for deciphering the action mechanism of herbal formula Zuojin Pill in suppressing hepatocellular carcinoma. Front Pharmacol. 2019;10:1–21. doi: https://doi.org/10.3389/fphar.2019.01185
63. Arif R, Bukhari SA, Mustafa G, Ahmed S, Albeshr MF. Network pharmacology and experimental validation to explore the potential mechanism of *Nigella sativa* for the treatment of breast cancer. Pharmaceuticals (Basel). 2024;17(5):617. doi: https://doi.org/10.3390/ph17050617
64. Bischoff-Kont I, Fürst R. Benefits of ginger and its constituent 6-Shogaol in inhibiting inflammatory processes. Pharmaceuticals (Basel). 2021;14(6):1–19. doi: https://doi.org/10.3390/ph14060571
65. Li T, Pan D, Pang Q, Zhou M, Yao X, Yao X, *et al.* Diarylheptanoid analogues from the rhizomes of *Zingiber officinale* and their anti-tumour activity. RSC Adv. 2021;11(47):29376–84. doi: https://doi.org/10.1039/d1ra03592d
66. Ganapathy G, Preethi R, Moses JA, Anandharamakrishnan C. Diarylheptanoids as nutraceutical: a review. Biocatal Agric Biotechnol. 2019;19:1–14. doi: https://doi.org/10.1016/j.bcab.2019.101109
67. Savaringal JP, Sanalkumar KB. Anti-ulcer effect of extract of rhizome of *Curcuma longa.* L against aspirin-induced peptic ulcer in rats. Natl J Physiol Pharm Pharmacol. 2018;8(5):650. doi: https://doi.org/10.5455/njppp.2018.8.1249201012018
68. Tao QF, Xu Y, Lam RYY, Schneider B, Dou H, Leung PS, *et al.* Diarylheptanoids and a monoterpenoid from the rhizomes of *Zingiber officinale*: antioxidant and cytoprotective properties. J Nat Prod. 2008;71(1):12–7. doi: https://doi.org/10.1021/np070114p
69. Huang Y, He C, Hu Z, Chu X, Zhou S, Hu X, *et al.* The beneficial effects of alpha-tocopherol on intestinal function and the expression of tight junction proteins in differentiated segments of the intestine in piglets. Food Sci Nutr. 2023;11(2):677–87. doi: https://doi.org/10.1002/fsn3.3103
70. Ajith TA, Nivitha V, Usha S. *Zingiber officinale* Roscoe alone and in combination with α-tocopherol protect the kidney against cisplatin-induced acute renal failure. Food Chem Toxicol. 2007;45(6):921–7. doi: https://doi.org/10.1016/j.fct.2006.11.014
71. Arefpour H, Sadeghi A, Zayeri F, Hekmatdoost A. The application of ginger supplementation on peptic ulcer disease management: a randomized, double blind, placebo-controlled clinical trial. Clin Nutr Open Sci. 2024;57:231–40. doi: https://doi.org/10.1016/j.nutos.2024.08.008
72. Huh E, Choi JG, Noh D, Yoo H-S, Ryu J, Kim N-J, *et al.* Ginger and 6-Shogaol protect intestinal tight junction and enteric dopaminergic neurons against 1-Methyl-4-Phenyl 1,2,3,6-Tetrahydropyridine in mice. Nutr Neurosci. 2020;23(6):455–64. doi: https://doi.org/10.1080/1028415X.2018.1520477
73. Kim Y, Kim D-M, Kim JY. Ginger extract suppresses inflammatory response and maintains barrier function in human colonic epithelial Caco-2 cells exposed to inflammatory mediators. J Food Sci. 2017;82(5):1264–70. doi: https://doi.org/10.1111/1750-3841.13695
74. Glaviano A, Foo ASC, Lam HY, Yap KCH, Jacot W, Jones RH, *et al.* PI3K/AKT/mTOR signaling transduction pathway and targeted therapies in cancer. Mol Cancer. 2023;22(1):1–37. doi: https://doi.org/10.1186/s12943-023-01827-6
75. Duggal S, Jailkhani N, Midha MK, Agrawal N, Rao KVS, Kumar A. Defining the Akt1 interactome and its role in regulating the cell cycle. Sci Rep. 2018;8(1):1–16. doi: https://doi.org/10.1038/s41598-018-19689-0
76. Sierra JC, Asim M, Verriere TG, Piazuelo MB, Suarez G, Romero-Gallo J, *et al.* Epidermal growth factor receptor inhibition downregulates *Helicobacter pylori*-induced epithelial inflammatory responses, DNA damage and gastric carcinogenesis. Gut. 2018;67(7):1247–60. doi: https://doi.org/10.1136/gutjnl-2016-312888
77. Shi Y-Y, Liu H-F, Min M, Wang W, Li J, He C-Y, *et al.* Correlation analysis of mast cells and EGFR with endoscopic application of tissue glue for treatment of peptic ulcer healing. Eur Rev Med Pharmacol Sci. 2017;21(4):861–6.
78. Luettig J, Rosenthal R, Lee I-FM, Krug SM, Schulzke JD. The ginger component 6-Shogaol prevents TNF-α-induced barrier loss via inhibition of PI3K/Akt and NF-κB signaling. Mol Nutr Food Res. 2016;60(12):2576–86. doi: https://doi.org/10.1002/mnfr.201600274
79. Mirza Z, Karim S. Structure-based profiling of potential phytomolecules with AKT1 a key cancer drug target. Molecules. 2023;28(6):1–14. doi: https://doi.org/10.3390/molecules28062597
80. Noor JJ, Sindhu R, Jothi AB, Prabu D, Mohan MR, Dhamodhar D, *et al.* Modulatory effects of gingerol in cancer cell growth through activation and suppression of signal pathways in cancer cell growth systemic review. J Pharm Bioallied Sci. 2024;16(Suppl 5):S4314–9. doi: https://doi.org/10.4103/jpbs.jpbs_1001_24
81. Liu Y, Li Y, Yuan Y-Y, Geng Z-P, Li J-L, Wang M-J, *et al.* Elucidation of the potential molecular mechanism of the active compounds of

Bryophyllum pinnatum (L. f.) Oken against gastritis based on network pharmacology. Chin J Anal Chem. 2023;51(1):1–11. doi: https://doi.org/10.1016/j.cjac.2022.100193
82. Kang BW, Chau I. Molecular target: pan-AKT in gastric cancer. ESMO Open. 2020;5(5):1–10. doi: https://doi.org/10.1136/esmoopen-2020-000728
83. Hisamatsu Y, Oki E, Otsu H, Ando K, Saeki H, Tokunaga E, *et al.* Effect of EGFR and p-AKT overexpression on chromosomal instability in gastric cancer. Ann Surg Oncol. 2016;23(6):1986–92. doi: https://doi.org/10.1245/s10434-016-5097-3
84. Luparello C. Cadmium-associated molecular signatures in cancer cell models. Cancers (Basel). 2021;13(11):1–18. doi: https://doi.org/10.3390/cancers13112823
85. Xue Q, Liu X, Chen C, Zhang X, Xie P, Liu Y, *et al.* Erlotinib protests against LPS-induced parthanatos through inhibiting macrophage surface TLR4 expression. Cell Death Discov. 2021;7(1):1–9. doi: https://doi.org/10.1038/s41420-021-00571-4
86. Li N, Tang B, Jia Y, Zhu P, Zhuang Y, Fang Y, *et al. Helicobacter pylori* CagA protein negatively regulates autophagy and promotes inflammatory response via c-Met-PI3K/Akt-mTOR signaling pathway. Front Cell Infect Microbiol. 2017;7(417):1–15. doi: https://doi.org/10.3389/fcimb.2017.00417
87. Sierra JC, Asim M, Verriere TG, Piazuelo MB, Suarez G, Romero-Gallo J, *et al.* Epidermal growth factor receptor inhibition downregulates *Helicobacter pylori*-induced epithelial inflammatory responses, DNA damage and gastric carcinogenesis. Gut. 2017;6(7):1247–60. doi: https://doi.org/10.1136/gutjnl-2016-312888
88. Thung I, Aramin H, Vavinskaya V, Gupta S, Park JY, Crowe SE, *et al.* Review article: the global emergence of *Helicobacter pylori* antibiotic resistance. Aliment Pharmacol Ther. 2016;43(4):514–33. doi: https://doi.org/10.1111/apt.13497
89. Ghasemian A, Fattahi A, Shokouhi Mostafavi SK, Almarzoqi AH, Memariani M, Ben Braiek O, *et al.* Herbal medicine as an auspicious therapeutic approach for the eradication of *Helicobacter pylori* infection: a concise review. J Cell Physiol. 2019;234(10):16847–60. doi: https://doi.org/10.1002/jcp.28363
90. Xue P, Sang R, Li N, Du S, Kong X, Tai M, *et al.* A new approach to overcoming antibiotic-resistant bacteria: traditional Chinese medicine therapy based on the gut microbiota. Front Cell Infect Microbiol. 2023;13:1–13. doi: https://doi.org/10.3389/fcimb.2023.1119037
91. Ebrahimi Z, Masoodi M, Aslani Z, Naghshi S, Khalighi Sikaroudi M, Shidfar F. Association between dietary antioxidant index and risk of *Helicobacter pylori* infection among adults: a case–control study. BMC Gastroenterol. 2022;22(413):1–7. doi: https://doi.org/10.1186/s12876-022-02488-3
92. Moonwiriyakit A, Pathomthongtaweechai N, Steinhagen PR, Chantawichitwong P, Satianrapapong W, Pongkorpsakol P. Tight junctions: from molecules to gastrointestinal diseases. Tissue Barriers. 2023;11(2):114–46. doi: https://doi.org/10.1080/21688370.2022.2077620
93. Chang K-W, Kuo C-Y. 6-Gingerol modulates proinflammatory responses in dextran sodium sulfate (DSS)-treated Caco-2 cells and experimental colitis in mice through adenosine monophosphate-activated protein kinase (AMPK) activation. Food Funct. 2015;6(10):3334–41. doi: https://doi.org/10.1039/C5FO00513B
94. Chen L, Shao J, Luo Y, Zhao L, Zhao K, Gao Y, *et al.* An integrated metabolism *in vivo* analysis and network pharmacology in UC rats reveal anti-ulcerative colitis effects from *Sophora flavescens* EtOAc extract. J Pharm Biomed Anal. 2020;186:1–12. doi: https://doi.org/10.1016/j.jpba.2020.113306
95. Nam H-H, Kim JS, Lee J, Seo YH, Kim HS, Ryu SM, *et al.* Pharmacological effects of *Agastache rugosa* against gastritis using a network pharmacology approach. Biomolecules. 2020;10(9):1–18. doi: https://doi.org/10.3390/biom10091298
96. Peng C, Ouyang Y, Lu N, Li N. The NF-κB signaling pathway, the microbiota, and gastrointestinal tumorigenesis: recent advances. Front Immunol. 2020;11:1–13. doi: https://doi.org/10.3389/fimmu.2020.01387
97. Tjandrawinata RR, Cahyana AH, Nugroho AO, Adi IK, Talpaneni JSR. Structure identification and risk assurance of unknown impurities in pramipexole oral drug formulation. Adv Pharmacol Pharm Sci. 2024;2024:1–12. doi: https://doi.org/10.1155/2024/5583526
98. Du X, Li Y, Xia Y-L, Ai S-M, Liang J, Sang P, *et al.* Insights into protein–ligand interactions: mechanisms, models, and methods. Int J Mol Sci. 2016;17(2):1–34. doi: https://doi.org/10.3390/ijms17020144
99. Liu T, Liu J, Hao L. Network pharmacological study and molecular docking analysis of Qiweitangping in treating diabetic coronary heart disease. Evid Based Complement Alternat Med. 2021;2021:1–10. doi: https://doi.org/10.1155/2021/9925556

How to cite this article:
Simatupang ST, Dermawan D, Nadia, Tan S, Tjandrawinata RR. Network pharmacology and molecular dynamics studies unveil the therapeutic mechanisms of *Zingiber officinale* against dyspepsia. J Appl Pharm Sci. 2025. Article in Press.
http://doi.org/10.7324/JAPS.2025.240961

SUPPLEMENTARY MATERIAL

The supplementary material can be accessed at the link here: [https://japsonline.com/admin/php/uploadss/4652_pdf.pdf]